Ockham's Razor for Paring Microkinetic Mechanisms: Electrical Analogy vs. Campbell's Degree of Rate Control

Patrick D. O'Malley and Ravindra Datta
Dept.of Chemical Engineering, Fuel Cell Center, Worcester Polytechnic Inst., Worcester, MA 01609

Saurabh A. Vilekar
Precision Combustion, Inc., 410 Sackett Point Road, North Haven, CT 06514

DOI 10.1002/aic.14956
Published online August 1, 2015 in Wiley Online Library (wileyonlinelibrary.com)

Elucidation of the key molecular steps and pathways in an overall reaction is of central importance in developing a better understanding of catalysis. Campbell's degree of rate control (DRC) is the leading methodology currently available for identifying the germane steps and key intermediates in a catalytic mechanism. We contrast Campbell's DRC to our alternate new approach involving an analysis and comparison of the "resistance" and de Donder "affinity," that is, the driving force, of the various steps and pathways in a mechanism, in a direct analogy to electrical networks. We show that our approach is as just rigorous and more insightful than Campbell's DRC. It clearly illuminates the bottleneck steps within a pathway and allows one to readily discriminate among competing pathways. The example used for a comparison of these two methodologies is a DFT study of the water–gas shift reaction on Pt–Re catalyst published recently.
 AIChE J, 61: 4332–4346, 2015
Keywords: Campbell's degree of rate control, mechanism reduction, sensitivity analysis, water–gas shift reaction, reaction route graph analysis, reaction affinity, reaction resistance

Introduction

A detailed understanding of the molecular mechanism of an overall reaction (OR) is of great importance in many fields including catalysis,[1–4] combustion,[5–7] environmental pollution,[8–10] and metabolic modeling.[11] However, assembling a comprehensive molecular mechanism, complete with associated kinetic and thermochemical parameters, is a formidable task, given the often enormous number of possible steps and molecular intermediates. For instance, the GRI 3.0 mechanism for methane combustion[12] includes 325 reaction steps among 53 species.

Emulating such extensive gas-phase kinetic models, now in common usage in air pollution and combustion modeling, for example, via CHEMKIN,[7] catalytic reaction mechanisms are also becoming increasingly impressive in size, from dozens of steps[13–15] to over a hundred.[16] This, despite the fact that accurate prediction of kinetic and thermodynamic parameters on a given catalyst based on first-principles[17–19] and/or semi-empirical[20,21] approaches is a significantly more daunting task than it is for gas-phase reactions. Typically, via the microkinetic approach,[1,22–24] these step kinetics are incorporated in species mass balance differential equations for a given reactor, and solved numerically for the unknown concentrations of the surface intermediates, from which the individual rate of each step as well as that of the OR is obtained. The numerical predictions may be finally compared to experimental data, for example, in a parity plot under a variety of operating conditions,[25] to determine if the proposed mechanistic steps and their computed kinetics are valid.

This modern computational "blackbox" approach is in stark contrast with the classical Langmuir–Hinshelwood–Hougen–Watson (LHHW) approach,[26,27] in which, somewhat arbitrarily, a single rate-determining step (RDS) is assumed, the remaining steps being at quasi-equilibriums (QE). If the resulting LHHW rate expression with fitted rate and equilibrium parameters agrees with experiments, the RDS is deemed valid.[28]

There is needed a middle ground between these two extremes that retains the rigor of modern predictive approach but endows it with insight to make the analysis and subsequent mechanism reduction more transparent. We describe such an approach here.

Whether the postulated molecular and kinetic complexity of a microkinetic network is justified in reality is, thus, an open and important question. In other words, it is much easier to propose a mechanistic step than to dispose-off one. Conversely, the parsimonious Ockham's razor[29] would recommend the simplest mechanism that can explain observations. For instance, Lu and Law[30] were able to reduce the complex GRI 3.0[12] from 325 down to a 15-step mechanism, which was found to be accurate in its predictions over a broad range of conditions. Such reduction, if done insightfully, is, of course, very desirable, as kinetic systems are often computationally challenging,[31] especially when coupled with transport equations, as in microkinetics,[1,25] or in computational fluid dynamics. If key steps could be identified, the researchers could

Correpondence concerning this article should be addressed to R. Datta at rdatta@wpi.edu.

devote more of their energies to accurately characterizing their kinetic/thermodynamic parameters, and focus on these in the design of more active and/or selective catalysts.[32]

Some of the tools that are currently in use for simplifying complex catalytic chemistry models include: (1) a pictorial comparison of the energy landscape of different pathways for pathway discrimination,[25] (2) a comparison of step reversibility, as proposed by Dumesic,[33] and (3) evaluation of Campbell's degree of rate control (DRC)[34–37] for identifying important steps and dominant surface intermediates.

The first of these, although intuitively appealing, is a qualitative graphical tool, while the second, involves only a thermodynamic criterion, not kinetic.[35,38] The most rigorous tool available so far is Campbell's DRC, which involves evaluating a normalized differential change in the rate of the OR, r_{OR}, for a normalized differential change in the forward rate constant of a given step s_ρ, holding invariable all step equilibrium constants and all other step rate constants, that is, $(X_{DRC,\rho} = \partial \ln r_{OR}/\partial \ln \vec{k}_\rho)_{K_\rho, \vec{k}_{r\neq\rho}}$. Campbell's DRC is powerful and derives from the broader concept of parametric sensitivity used widely in the analysis of kinetic and reactor systems.[3,7,39,40] However, it is a "black box" numerical approach.

Here, we discuss an alternate approach based on electrical network analogy of a reaction mechanism within the reaction route (RR) graph analysis approach[41–44] developed by us, which involves an evaluation of the reaction step "affinity," or driving force, and "resistance" under a variety of conditions. It is just as rigorous and substantially more revealing than Campbell's DRC, allowing transparent pruning of complex catalytic reaction networks. The example that we use for this study involves the DFT study of the water–gas shift (WGS) reaction on Pt–Re. It is shown that while Campbell's DRC leads to erroneous conclusions for this example, our approach allows rigorous mechanism analysis and reduction, eventually leading to a simplified but accurate rate law.

An expansive starting mechanism is, of course, not necessarily exhaustive, and could well miss one or more critical steps. One does not know *a priori* which elementary steps really occur, and which are the real intermediates. The intermediates are generally too fleeting to be detected via spectroscopic techniques, so that one has to depend on quantum mechanical methods for insights. However, these are extremely time consuming for an exhaustive search. Therefore, one is limited by pointers in the literature and one's own chemical intuition to assemble a good mechanism, followed by use of DFT to find their energetics. Clearly, however, there is a risk that an important reaction is overlooked. The approach presented here, of course, cannot overcome any such deficiency of a given mechanism. It is, thus, only an ex post method to check the consistency of the network found by experimental and DFT procedures, and as a useful tool for reducing/pruning the assembled network.

Theory

As Campbell's DRC is a form of parametric sensitivity analysis, we start below with a discussion of the latter first.

Parametric sensitivity analysis

Consider a system (e.g., a catalyst, or a catalytic reactor), as shown schematically in Figure 1, characterized by its steady-state "response" variable $y_j = y_j(\mathbf{a})$ (e.g., conversion, selectivity, composition of a reactant or a product, the rate of the OR, or the rate of generation/consumption of a species, etc.), which

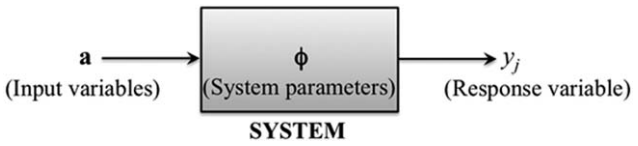

Figure 1. A chemical system (e.g., a catalyst) as a (black) box, with response (*r*), for example, conversion or OR rate, determined by input variables (e.g., species composition vector, a) and system parameters (e.g., step activation energy vector, ϕ).

may be an explicit expression, a numerical solution, or simply tabular data, where $\boldsymbol{\phi}$ is a vector of p independent system parameters, (e.g., step rate constants, pre-exponential factors, or activation barriers, etc.), and $\mathbf{a}$ is a vector of n input, or "imposed," variables (e.g., species activities, temperature, pressure, flow rate, etc).

The total differential change in the response variable y_j due to incremental changes in all system parameters ϕ_ρ ($\rho = 1, 2, \ldots, p$)

$$dy_j(\mathbf{a}) = \frac{\partial y_j}{\partial \phi_1} d\phi_1 + \frac{\partial y_j}{\partial \phi_2} d\phi_2 + \cdots + \frac{\partial y_j}{\partial \phi_\rho} d\phi_\rho + \cdots + \frac{\partial y_j}{\partial \phi_p} d\phi_p = \sum_{\rho=1}^{p} S_{y_j,\phi_\rho} d\phi_\rho \tag{1}$$

where the absolute local sensitivity coefficient is defined as

$$S_{y_j,\phi_\rho}(\mathbf{a}, \phi_\rho) \equiv \frac{\partial y_j(\mathbf{a}, \phi_\rho)}{\partial \phi_\rho} = \lim_{\Delta\phi_\rho \to 0} \frac{y_j(\mathbf{a}, \phi_\rho + \Delta\phi_\rho) - y_j(\mathbf{a}, \phi_\rho)}{\Delta\phi_\rho} \tag{2}$$

which may be an analytical expression if y_j is an explicit expression,[3] or a numerical, or even an experimental value, and depends on the input variables vector $\mathbf{a}$ and the balance system parameters in $\boldsymbol{\phi}$ that remain unchanged.

As an aside, the local sensitivity coefficients may also be used, along with an estimate of the uncertainty in each parameter, σ_ρ, for example, those of the rate constants in their DFT estimation,[45] to obtain the overall uncertainty in the response variable, via an estimate of its variance,[9] i.e., $\sigma_{y_j}^2(\mathbf{a}) = \sum_{\rho=1}^{p} \left(\frac{\partial y_j}{\partial \phi_\rho}\right)^2 \sigma_\rho^2 = \sum_{\rho=1}^{p} S_{y_j,\phi_\rho}^2 \sigma_\rho^2$ where each term in the summation is an estimate of the contribution of the uncertainty in each parameter ϕ_ρ to the overall uncertainty in the response variable y_j.

It is, however, often preferable to define an alternate normalized (or a relative) local sensitivity coefficient

$$X_{y_j,\phi_\rho}(\mathbf{a}, \phi_\rho) \equiv \frac{\phi_\rho}{y_j} \cdot \frac{\partial y_j(\mathbf{a}, \phi_\rho)}{\partial \phi_\rho} = \frac{\partial \ln y_j(\mathbf{a}, \phi_\rho)}{\partial \ln \phi_\rho} = \frac{\phi_\rho}{y_j} \cdot S_{y_j,\phi_\rho}(\mathbf{a}, \phi_\rho) \tag{3}$$

in which the parameter ϕ_ρ as well as the response function y are normalized, so that it has the additional virtue of being dimensionless.

Once computed, these p sensitivity indices may be written as a row normalized sensitivity coefficient vector

$$\mathbf{X}_j^T(\mathbf{a}, \phi_\rho) = \begin{pmatrix} X_{y_j,\phi_1} & X_{y_j,\phi_2} & \cdots & X_{y_j,\phi_p} \end{pmatrix} = \begin{pmatrix} \frac{\partial \ln y_j}{\partial \ln \phi_1} & \frac{\partial \ln y_j}{\partial \ln \phi_2} & \cdots & \frac{\partial \ln y_j}{\partial \ln \phi_p} \end{pmatrix} \tag{4}$$

Furthermore, as above, from the definition of the total derivative for y_j

$$d\ln y_j = \sum_{\rho=1}^{p} \left(\frac{\partial \ln y_j}{\partial \ln \phi_1} \right) d\ln \phi_\rho = \sum_{\rho=1}^{p} X_{y_j,\phi_\rho} d\ln \phi_\rho \tag{5}$$

Campbell's DRC

The generic parametric sensitivity coefficient defined above is of broad utility in a variety of fields.[6–11] Conversely, Campbell's DRC[34–36] is a specialized version developed for use in pruning microkinetic models in catalysis, with the following stipulations: (1) it is defined as the normalized sensitivity coefficient of the rate of the OR (i.e., the response variable, $y_j = r_{\mathrm{OR}}$) with respect to (2) the forward rate constant of step s_ρ, (i.e., the system parameter, $\phi_\rho = \vec{k}_\rho$), while (3) holding constant all other step rate constants, as well as (4) all step equilibrium constants (including that of the step s_ρ), that is

$$\begin{aligned} X_{\mathrm{DRC},\rho}(\mathbf{a}, \vec{k}_\rho) &\equiv \frac{\vec{k}_\rho}{r_{\mathrm{OR}}} \cdot \left(\frac{\partial r_{\mathrm{OR}}}{\partial \vec{k}_\rho} \right)_{\mathbf{a},K_\rho,\vec{k}_{r\neq\rho}} \\ &= \left(\frac{\partial \ln r_{\mathrm{OR}}}{\partial \ln \vec{k}_\rho} \right)_{\mathbf{a},K_\rho,\vec{k}_{r\neq\rho}} = \left\{ \frac{\partial \ln r_{\mathrm{OR}}}{\partial(-\Delta \vec{G}_\rho^{\ddagger,\mathrm{o}}/RT)} \right\}_{\mathbf{a},K_\rho,\vec{k}_{r\neq\rho}} \end{aligned} \tag{6}$$

Here, the last equality stems from the thermodynamic transition-state theory (TTST) relation for the rate constant, that is, $\vec{k}_\rho = \kappa(k_{\mathrm{B}}T/h)\exp(-\Delta \vec{G}_\rho^{\ddagger,\mathrm{o}}/RT)$, where $\Delta \vec{G}_\rho^{\ddagger,\mathrm{o}}$ is the Gibbs free energy (GFE) of activation for the forward step. Furthermore, as $\Delta \vec{G}_\rho^{\ddagger,\mathrm{o}} = \Delta \vec{H}_\rho^{\ddagger,\mathrm{o}} - T\Delta \vec{S}_\rho^{\ddagger,\mathrm{o}} \cong \vec{E}_\rho - T\Delta \vec{S}_\rho^{\ddagger,\mathrm{o}}$, the differential change in $\ln \vec{k}_\rho$ may be brought about by incrementally changing the activation energy $\vec{E}_\rho$ of the step s_ρ, holding the entropy of activation $\Delta \vec{S}_\rho^{\ddagger,\mathrm{o}}$ constant.[36]

The key aspect, thus, that distinguishes Campbell's DRC from simply being the normalized sensitivity coefficient with respect to the forward rate constant,[8] is that the thermodynamics of the step s_ρ, are not altered in Campbell's DRC as $\vec{k}_\rho$ is varied incrementally, so that $\overleftarrow{k}_\rho$ changes concomitantly such that $\Delta \vec{k}_\rho / \vec{k}_\rho = \Delta \overleftarrow{k}_\rho / \overleftarrow{k}_\rho$. This is so because the equilibrium constant that is held constant for the elementary step and its forward and reverse rate constants are interrelated via the TTST relation

$$K_\rho = \exp\left(-\frac{\Delta G_\rho^{\mathrm{o}}}{RT} \right) = \exp\left(-\frac{\Delta \vec{G}_\rho^{\ddagger,\mathrm{o}} - \Delta \overleftarrow{G}_\rho^{\ddagger,\mathrm{o}}}{RT} \right) = \frac{\vec{k}_\rho}{\overleftarrow{k}_\rho} \tag{7}$$

Furthermore, the GFE of activation for the forward step in Eq. 6 is

$$\Delta \vec{G}_\rho^{\ddagger,\mathrm{o}} \equiv G_{f,\rho}^{\ddagger,\mathrm{o}} + \sum_{i=1}^{n} \nu_{\rho i} G_{f,i}^{\mathrm{o}} \tag{8}$$

where $G_{f,\rho}^{\ddagger,\mathrm{o}}$ is the standard (for unit activity) GFE of formation of the transition-state complex (TSC) of step s_ρ, $G_{f,i}^{\mathrm{o}}$ is that of the reactant species i in step s_ρ, and $\nu_{\rho i}$ is the stoichiometric coefficient of species i in step s_ρ (by convention, $\nu_{\rho i} < 0$ for reactants and $\nu_{\rho i} > 0$ for products).

It is assumed next that the incremental change in $\Delta \vec{G}_\rho^{\ddagger,\mathrm{o}}$ in Eq. 6 is brought about by incrementally perturbing the standard GFE of formation of the TSC of step s_ρ, that is, $G_{f,\rho}^{\ddagger,\mathrm{o}}$, rather than that of any of the reactant species $G_{f,i}^{\mathrm{o}}$ in the step s_ρ. Then, Campbell's DRC, Eq. 6, may alternately be written in the form[36]

$$X_{\mathrm{DRC},\rho} = \left\{ \frac{\partial \ln r_{\mathrm{OR}}}{\partial(-G_{f,\rho}^{\ddagger,\mathrm{o}}/RT)} \right\}_{\mathbf{a},G_{f,i}^{\mathrm{o}},G_{f,r\neq\rho}^{\ddagger,\mathrm{o}}} \tag{9}$$

where all other standard GFE of formation of species are held constant, as well as that for the TSCs of all other steps. The incremental change in the standard GFE of formation of the TSC may further be brought about by incrementally changing the standard enthalpy of formation of the TSC of the step, $H_{f,\rho}^{\ddagger,\mathrm{o}}$, holding the entropy of formation of the TSC $S_{f,\rho}^{\ddagger,\mathrm{o}}$ constant.[36]

An alternate way to view Eq. 9 is as a reaction forming the particular TSC from the reactants of the OR, or from terminal species, rather than from those in the step s_ρ, so that the Campbell's DRC may then be construed as a derivative with respect to the equilibrium constant of reaction of formation of the TSC of step ρ from the OR terminal reactants.[36] This may be accomplished by appropriately combining the elementary steps into the so-called intermediate reactions (IR).[41–43]

There are different ways in which the Campbell's DRC, once hence numerically computed for all the steps in a microkinetic model, may be utilized for identification of key steps and model reduction.[46] One such method is the so-called principal component analysis,[40,47,48] in which the eigenvalues and eigenvectors of the matrix $\mathbf{X}^T\mathbf{X}$ are computed. The dominant eigenvalues then indicate the principal eigenvectors, and the biggest elements of these eigenvectors provide the most significant steps in the mechanism.

A second approach is to simply compare Campbell's DRC of a given step as a fraction of its sum for all steps, where the latter may be obtained from Eqs. 5 and 6, which for equal relative variation of the rate constants (i.e., for $d\vec{k}_1/\vec{k}_1 = d\vec{k}_2/\vec{k}_2 = \cdots d\vec{k}_\rho/\vec{k}_\rho \equiv d\vec{k}/\vec{k}$)

$$\frac{d\ln r_{\mathrm{OR}}}{d\ln \vec{k}} = \sum_{\rho=1}^{p} X_{\mathrm{DRC},\rho} \tag{10}$$

and describes the total normalized change in the OR rate as a result of an equal normalized differential change in the rate constants of all steps in a microkinetic mechanism.

In fact, it has been often conjectured[3,35,49] (based on some numerical examples, although not proven mathematically) that $\sum_{\rho=1}^{p} X_{\mathrm{DRC},\rho} = 1$. Therefore, Campbell[34,35] suggests simply comparing the absolute numerical value of the DRC for each step for model reduction and for identification of the RDS, if any. However, in more recent work, it has been found that the common assertion that $\sum_{\rho=1}^{p} X_{\mathrm{DRC},\rho} = 1$ is incorrect.[25]

At any rate, the larger the calculated value of $X_{\mathrm{DRC},\rho}$, the greater the degree of control that the step s_ρ exerts on the overall rate. A positive value for $X_{\mathrm{DRC},\rho}$ suggests that increasing the rate constant $\vec{k}_\rho$ would increase r_{OR}, so that the corresponding step s_ρ may be considered as a rate-limiting step (RLS). Conversely, a negative value for $X_{\mathrm{DRC},\rho}$ suggests an inhibiting step. A $X_{\mathrm{DRC},\rho} \to 0$ indicates a QE step. Conversely, a $X_{\mathrm{DRC},\rho} \to 1$ indicates a RDS. Once the key steps in a mechanism are hence identified, one can, in principle, design a better catalyst based on these insights.[32,37]

It is possible to generalize Campbell's sensitivity analysis approach to also determine the so-called degree of thermodynamic control (DTC) of a step,[36] defined, in analogy to Eq. 9, as

$$X_{\mathrm{DTC},k} \equiv \left\{ \frac{\partial \ln r_{\mathrm{OR}}}{\partial(-G^{\mathrm{o}}_{f,k}/RT)} \right\}_{\mathbf{a}, G^{\mathrm{o}}_{f,i\neq k}, G^{\ddagger,\mathrm{o}}_{f,\rho}} \tag{11}$$

where the relative change in the rate of the OR is evaluated in response to a small relative change in the standard-state GFE change of the step s_ρ, realized by changing the GFE of formation of the intermediate k in that step, holding constant all other GFE extrema (minima as well as saddle points in the energy landscape). Furthermore, as above, the GFE of formation in Eq. 11 may be written in terms of the equilibrium constant of an IR forming the desired intermediate from terminal species, by appropriately linearly combining the elementary steps.

In view of Eqs. 9 and 11, both the DRC and the DTC may be viewed from a common standpoint,[36] with the standard GFE of formation of the TSC being varied in the former, while the standard GFE of formation of the intermediate of interest being varied in the latter.

Stegelmann et al.[36] further conjectured (although also not proven mathematically), based on numerical examples, that the DTC is proportional to the surface coverage of the intermediate k

$$X_{\mathrm{DTC},k} = -\sigma \cdot \theta_k \tag{12}$$

with the proportionality constant σ varying typically between 1 and 2, being the number of sites involved in the RDS. Furthermore, they found that the DTC is always zero or negative, that is, rate remains unchanged or reduces when an intermediate is stabilized depending on whether or not it is a dominant species on the surface. Increasing the coverage of an already abundant surface intermediate can reduce OR rate by suppressing those of others further.

In summary, $X_{\mathrm{DRC},\rho}$ may be used to determine the kinetically significant TSCs in a microkinetic mechanism, while $X_{\mathrm{DTC},k}$ may be used for identifying the key reactive intermediates, that is, those that exert a dominant control on the rate of the OR. This then offers the potential of increasing the OR rate by changing the appropriate step energies through catalyst design.

As a practical matter in catalyst design, of course, it is not possible to simply change GFE of one transition state or of one intermediate and nothing else.[37] The GFE of activation and that of a step are, in fact, related via the commonly observed linear-free energy relation[50]

$$\frac{d(\Delta \vec{G}^{\ddagger,\mathrm{o}}_{\rho})}{d(\Delta G^{\mathrm{o}}_{\rho})} = \beta_\rho \tag{13}$$

Other such relations that describe the commonly observed interrelation between kinetics and thermodynamics are the Brønsted–Evans–Polanyi–Semenov relation,[3,51] $d(\vec{E}_\rho) = \beta_\rho d(\Delta H^{\mathrm{o}}_\rho)$.

Electrical analogy and reaction networks

A virtue of Campbell's DRC is that it is general tool of microkinetic model reduction, that is, without regard to the degree of complexity of a molecular mechanism, which may involve multiple parallel pathways. However, a limitation is that it is simply a numerical sensitivity analysis tool for a chemical system treated as a proverbial "black box" (Figure 1).

Conversely, Horiuti provided an alternate criterion for identifying the RDS in a sequence,[33,52] that is, the RDS is the only exergic step ($A_\rho = -\Delta G_\rho > 0$, where A_ρ is the de Donder affinity) in a sequence, the remaining steps being at QE ($A_\rho \to 0$). However, the step affinity is simply its thermodynamic driving force, akin to voltage across an electrical element in an electrical circuit, the rate (current) of a step (electrical element) being also determined by its kinetics (resistance) as well. Furthermore, of course, there can be, and often is, more than one step with $A_\rho > 0$.[52]

Thus, identification of significant steps simply based on perturbation of the rate constant or activation barriers, as via Campbell's DRC,[35] or alternately based on simply the thermodynamic driving force, the de Donder affinity,[33,52] both provide only a partial perspective, as the net rate of a step involves both kinetics and thermodynamics, that is

$$r_\rho = \vec{r}_\rho - \overleftarrow{r}_\rho = \vec{r}_\rho(1 - z_\rho) = \vec{r}_\rho(1 - e^{-\mathcal{A}_\rho}) \tag{14}$$

where $z_\rho \equiv \overleftarrow{r}_\rho / \vec{r}_\rho$ is the step reversibility,[33] and $\mathcal{A}_\rho = A_\rho/RT$ is dimensionless de Donder affinity, while $A_\rho = -\Delta G_\rho$ is the de Donder affinity for reaction step s_ρ.[53]

In other words, one needs both thermodynamic (affinity, or reversibility) and kinetic (resistance) characteristics of a reaction step to judge its significance in the overall scheme of things. The electrical network analogy based on the RR graph approach[41–43] incorporates both of these aspects. It, thus, comprehensively incorporates and illuminates the network structural constraints embodied by the two Kirchhoff's laws (mass balance, and Hess's law) described below, which further ascribe to reaction networks a complete and quantitative correspondence to electrical networks. Furthermore, the pictorial representation of the reaction network not only provides the corresponding electrical circuit but also makes abundantly clear which pathways and steps are dominant and which may be neglected. It is, thus, a comprehensive and a transparent approach. For its application, however, one first needs the complete, or at least its simplified version, RR graph, obtained for a given mechanism as described below.

The RR Graph and the Electrical Analogy. The RR graph of a mechanism for an OR comprising of p reaction steps s_ρ among $q+1$ intermediate species and n terminal species (OR reactants and products), is a quantitative graph theoretical depiction of the reaction network, in which the steps as well as the OR, are represented individually as directed (arrows pointed in the assumed direction) branches, or edges, interconnected at nodes, or vertices, n_j, so that all RRs may be traced on it as closed walks, or cycles, and the nodal connectivity to branches is consistent with quasi-steady state (QSS) mass balance of one or a linear combination of species.

An example of a RR graph is shown in Figure 2, which, as described below, is the RR graph for the WGS mechanism on Pt–Re provided in Table 1. Once the RR graph of a mechanism is obtained, the equivalent electrical network is obtained simply by replacing the individual branches by their step resistances, and the OR by an electromotive force (EMF) providing the OR driving force of OR affinity, as shown in Figure 3 for the WGS example.

While, graphically, an RR is a closed walk starting and ending at the same node, mathematically, it is a linear combination of reaction steps, $\mathrm{RR}_g: \sum_\rho \sigma_{g\rho} s_\rho = 0$. Here, $\sigma_{g\rho}$ is stoichiometric number (usually, 0, ± 1, or ± 2) of step s_ρ in the gth RR, which provides the number and direction of a step in a walk. Mathematically, $\sigma_{g\rho}$ is determined from the requirement to eliminate all species, intermediate as well as terminal, in a RR. When the reaction steps involved in a RR do not include the OR, then the RR is called an empty route (ER). When the

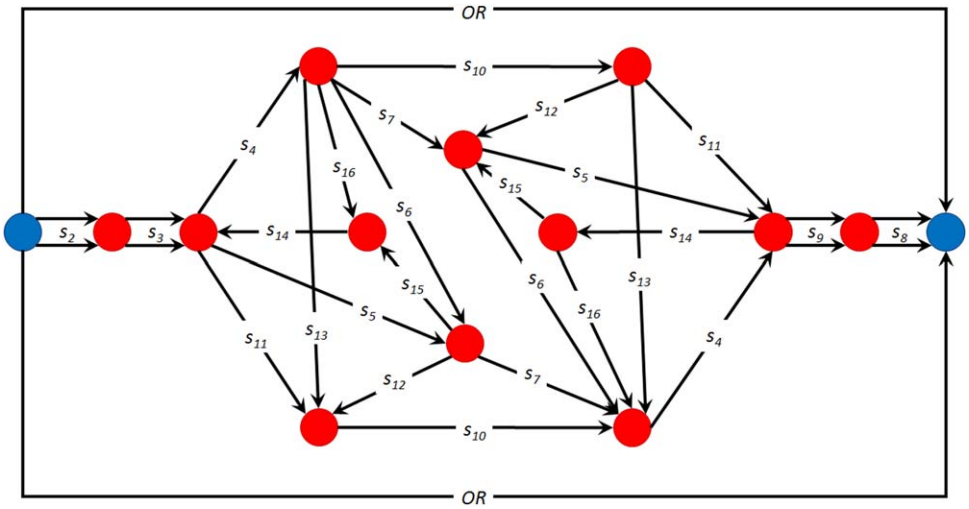

Figure 2. Complete RR graph for the WGS reaction on Pt–Re with mechanism given in Table 1.

[Color figure can be viewed in the online issue, which is available at wileyonlinelibrary.com.]

OR is included, then the RR is a full route (FR). In fact, subtracting one FR from another results in an ER, because the OR gets cancelled in the process. Furthermore, note that mathematically the sequence of steps is arbitrary.

There are, however, some walks that are not closed, that is, they start and end at different nodes. These are called intermediate reaction routes. In these, not all species are eliminated. Thus, the resulting IR, typically includes both terminal species and specified intermediate species.

As per the Horiuti–Temkin theorem, furthermore, an independent RR set is any set of $\mu = p - q$ RRs, which may include any FRs and ERs, so long as they include among them all of the steps in the mechanism. Moreover, the number of linearly independent ERs is given by $\mu - 1 = p - (q + 1)$. In other words, any set of RRs (ERs and FRs) that includes all the steps including the OR is an appropriate independent set, for example, an appropriate set is $\mu - 1$ ERs and one FR.

As indicated above, the RR graph is a useful, quantitative, graph-theoretical representation of the molecular mechanism that provides: (1) consistence of nodes with species mass balance, that is, Kirchhoff's Flux Law (KFL), alternately, Kirchhoff's First Law, that is, the QSS assumption of kinetics, or the Bodenstein approximation; (2) consistence of RRs with the state-property of thermodynamic functions (e.g., GFE, G, enthalpy H, and entropy S), that is, Kirchhoff's potential law (KPL), also called Kirchhoff's second law, alternately known as Hess's law, according to which change in a thermodynamic state property along a cycle is zero; (3) graphical enumeration of all possible RRs as closed walks, normally done from stoichiometric analysis;[53] and (4) minimality, or directness,[54] of both RRs as well as nodal degree, namely, the number of branches incident on a node.

It, actually, turns out that the second and third property above, that is, consistence with KPL and enumeration of RRs, are mathematically equivalent. In other words, a RR graph that is consistent with KPL is automatically amenable to a graph-theoretic enumeration of all RRs, and vice versa. As a result, we are concerned only with the two requirements of consistence with the two Kirchhoff's laws, along with their directness, that is, the number of steps involved in the KPL and KFL relations are minimal.

Drawing the RR Graph or Electrical Network. The first step in the use of the RR graph approach is, of course, to construct the RR graph or electrical network from a given mechanism. It turns out that this is often not a trivial matter, because of the fact that the three basic requirements, namely, KFL,

Table 1. The Considered Microkinetic Model for WGS on Pt–Re[58]

	$\vec{E}_\rho$	$\vec{\Lambda}_\rho$	Elementary Reactions	$\overleftarrow{E}_\rho$	$\overleftarrow{\Lambda}_\rho$	$\vec{\omega}_\rho$	$\overleftarrow{\omega}_\rho$
s_2:	0	1.00×10^{13}	$H_2O + S \rightleftarrows H_2O{\cdot}S$	0	1.00×10^{13}	$\vec{k}_2 p_{H_2O}$	$\overleftarrow{k}_2$
s_3:	0	1.00×10^{13}	$CO + S \rightleftarrows CO{\cdot}S$	0	3.30×10^{12}	$\vec{k}_3 p_{CO}$	$\overleftarrow{k}_3$
s_4:	44.16	1.00×10^{13}	$H_2O{\cdot}S + S \rightleftarrows OH{\cdot}S + H{\cdot}S$	44.16	7.89×10^{12}	$\vec{k}_4$	$\overleftarrow{k}_4$
s_5:	44.24	1.00×10^{13}	$OH{\cdot}S + S \rightleftarrows O{\cdot}S + H{\cdot}S$	42.24	9.88×10^{12}	$\vec{k}_5$	$\overleftarrow{k}_5$
s_6:	0	9.24×10^{12}	$2OH{\cdot}S \rightleftarrows H_2O{\cdot}S + O{\cdot}S$	0	7.53×10^{12}	$\vec{k}_6$	$\overleftarrow{k}_6$
s_7:	113.28	1.00×10^{13}	$CO{\cdot}S + O{\cdot}S \rightleftarrows CO_2{\cdot}S + S$	113.28	2.94×10^{13}	$\vec{k}_7$	$\overleftarrow{k}_7$
s_8:	0	1.00×10^{13}	$CO_2{\cdot}S \rightleftarrows CO_2 + S$	0	1.00×10^{13}	$\vec{k}_8$	$\overleftarrow{k}_8 p_{CO_2}$
s_9:	9.89	1.00×10^{13}	$2H{\cdot}S \rightleftarrows H_2 + 2{\cdot}S$	0	4.00×10^{10}	$\vec{k}_9$	$\overleftarrow{k}_9 p_{H_2}$
s_{10}:	2.88	1.00×10^{13}	$CO{\cdot}S + OH{\cdot}S \rightleftarrows COOH{\cdot}S + S$	2.88	3.23×10^{12}	$\vec{k}_{10}$	$\overleftarrow{k}_{10}$
s_{11}:	118.08	1.99×10^{12}	$COOH{\cdot}S + S \rightleftarrows CO_2{\cdot}S + H{\cdot}S$	66.24	9.89×10^{13}	$\vec{k}_{11}$	$\overleftarrow{k}_{11}$
s_{12}:	95.04	3.74×10^{12}	$COOH{\cdot}S + O{\cdot}S \rightleftarrows CO_2{\cdot}S + OH{\cdot}S$	95.04	4.97×10^{10}	$\vec{k}_{12}$	$\overleftarrow{k}_{12}$
s_{13}:	31.68	1.00×10^{13}	$COOH{\cdot}S + OH{\cdot}S \rightleftarrows CO_2{\cdot}S + H_2O{\cdot}S$	31.68	1.08×10^{12}	$\vec{k}_{13}$	$\overleftarrow{k}_{13}$
s_{14}:	90.24	1.00×10^{13}	$CO_2{\cdot}S + H{\cdot}S \rightleftarrows HCOO{\cdot}S{\cdot}S$	90.24	1.00×10^{13}	$\vec{k}_{14}$	$\overleftarrow{k}_{14}$
s_{15}:	175.68	1.00×10^{13}	$HCOO{\cdot}S{\cdot}S + O{\cdot}S \rightleftarrows CO_2{\cdot}S + OH{\cdot}S + S$	175.68	1.00×10^{13}	$\vec{k}_{15}$	$\overleftarrow{k}_{15}$
s_{16}:	128.64	1.65×10^{11}	$HCOO{\cdot}S{\cdot}S + OH{\cdot}S \rightleftarrows CO_2{\cdot}S + H_2O{\cdot}S + S$	128.64	1.00×10^{13}	$\vec{k}_{16}$	$\overleftarrow{k}_{16}$

The letter "S" is a surface site. Activation energies in kJ/mol; the units of the pre-exponential factors are $\text{atm}^{-1}\ \text{s}^{-1}$ for adsorption and desorption reactions and s^{-1} for surface reactions. ω_ρ is the reaction step weight in terms of rate constant, k and partial pressure of terminal species. The forward and reverse rate constants ($\vec{k}_\rho$ and $\overleftarrow{k}_\rho$, respectively) are calculated by: $\vec{k}_\rho = \vec{\Lambda}_\rho \exp\left(-\frac{\vec{E}_\rho}{RT}\right)$ and $\overleftarrow{k}_\rho = \overleftarrow{\Lambda}_\rho \exp\left(-\frac{\overleftarrow{E}_\rho}{RT}\right)$.

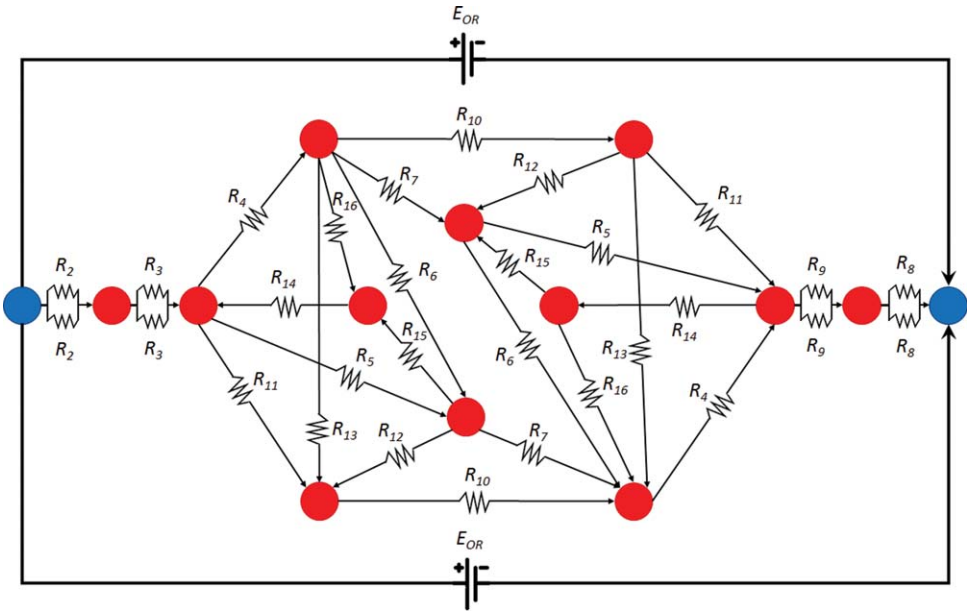

Figure 3. An electrical analogy for the WGS reaction on Pt-Re with mechanism given in Table 1.

[Color figure can be viewed in the online issue, which is available at wileyonlinelibrary.com.]

KPL, and minimality impose strict limitations on the topology of the resulting RR graph, so that often only a unique solution is admissible. We have so far found no more than two RR graphs for any reaction system. The preferred method to draw the RR graph for a given mechanism is to start with a set of independent cycles (KPL relations) that are drawn and combined in a way to ensure compatibility with KFL relations.

Thus, the recipe for drawing the RR graph is as follows[41]: (1) start with a set of independent RR matrix σ in which there is a single OR (or an independent number of ORs), and the remaining are ERs (ERs may be obtained by subtracting one FR from another other); (2) obtain a set of KFL relations by starting with the QSS relations for the individual species and linearly combining them to obtain a set with minimality ($\leq p - q + 1$); (3) draw the ERs as cycles, as well as the FR, with steps drawn as branches, interconnected at nodes; (4) combine ERs, one at a time, by merging common branches as far as one can go. The resulting sub-graph containing the ERs is called the cycle graph; (5) if a step is repeated in a RR, that is, if $\sigma_{g\rho}=+2$, then duplicate the cycle graph, flipping it on an axis; (6) fuse minimal number of nodes to merge the cycle graphs, ensuring that the fused nodes are also direct or minimal; (7) merge with the FR that includes the OR, to obtain the complete RR graph; and finally, (8) check to make sure that connectivity at all the nodes is consistent with appropriate KFL relations.

Finally, it should be remarked that the QSS analysis is used in our approach to obtain the KFL relations that provide the nodal connectivity of the RR graph. However, once determined, the RR graph can be used for the analysis of non-steady-state cases as well.

Kirchhoff's Laws and The Electrical Network Analogy. Since consistence with the two Kirchhoff's laws is central to the RR graph architecture, these are defined next, and impose important constraints on the kinetics and thermodynamics of reaction networks.

Thus, KFL implies that the branch rate, r_ρ (likened to branch current) of all branches incident at a node j sum up to zero, that is, $\Phi_j : \sum_\rho m_{\rho j} r_\rho = 0$, where the incidence coefficient $m_{\rho j}=+1$, if a branch leaves a node, and $m_{\rho j}=-1$, if a branch is coming into it.

KPL implies that a thermodynamic potential change across a branch ΔY_ρ, (e.g., ΔH_ρ, ΔG_ρ, or ΔS_ρ, likened to branch voltage drop) of all branches in a cycle or RR, sum up to zero, that is, $\sum_\rho \sigma_{g\rho} \Delta Y_\rho = 0$, where the stoichiometric number $\sigma_{g\rho}=+1$, if a branch is directed in the direction of the walk, and $\sigma_{g\rho}=-1$, if a branch is directed in the opposite direction.

The requirement of consistence with the two Kirchhoff's laws confers on the RR graphs a one-to-one correspondence with electrical circuits, which is a useful analogy because of the vast and well-grounded literature on circuit analysis.[55] Thus, the electrical analog of the RR graph is obtained by simply replacing the branches by resistors and the OR by an EMF, as shown in Figure 3.

Even though, the electrical analogy is complete without the following, for convenience, we may write the rate of a reaction step in the form of Ohm's law[41]

$$r_\rho \equiv \frac{\mathcal{A}_\rho}{R_\rho} \tag{15}$$

where $\mathcal{A}_\rho$ is the dimensionless step affinity akin to voltage in an electrical circuit. It is in turn related to the ratio of the rate in the forward direction $\vec{r}_\rho$ to that in the reverse direction, $\overleftarrow{r}_\rho$, via the de Donder relation[33,52]

$$\mathcal{A}_\rho = \ln\left(\frac{\vec{r}_\rho}{\overleftarrow{r}_\rho}\right) = \ln\left(\frac{1}{z_\rho}\right) \tag{16}$$

which stems from the thermodynamic consistence of elementary step kinetics, so that the step resistance, by combining the last two equations, is given by

$$R_\rho = \frac{\ln(\vec{r}_\rho / \overleftarrow{r}_\rho)}{\vec{r}_\rho - \overleftarrow{r}_\rho} \tag{17}$$

Clearly, unlike electrical resistance which is substantially constant, this definition of kinetic resistance of a step, strongly depends on reaction conditions, especially, temperature.

Now that the RR graph follows KFL, KPL, as well as Ohm's law, it is completely consistent with a resistive network.[55] Consequently, we can write the overall rate as the ratio of the affinity of the OR and the overall resistance of the reaction network

$$r_{OR} \equiv \frac{\mathcal{A}_{OR}}{R_{OR}} \tag{18}$$

where the OR resistance of the network is obtained in terms of the individual step resistances, in a manner similar to the electrical circuit.[55]

Use of the Electrical Analogy for Microkinetic Analysis and Pruning. To obtain the rates for the elementary steps as well as for the OR, one needs to first solve for the unknown intermediates concentrations θ_k ($k = 0, 1, 2, \ldots, q$), for which the number of relations needed are $(q + 1)$. One of these is always the mass balance of intermediates, for example, site balance, that is, site fractions add up to unity, $1 = \sum_{k=0}^{q} \theta_k$. The remaining are the q independent KFL relations applied to the nodes in the RR graph, which are essentially linear combinations of the q QSS relations, that is, the Bodenstein approximation that assumes that the concentrations of the intermediate species are invariant with time. In these are substituted step kinetics. We club together in the mass-action kinetics, the product of the known rate parameters and activities of terminal species into reaction weights, ω_ρ, leaving behind the rates explicitly in terms of the unknown intermediates concentrations and known ω_ρ.

The q KFL equations incorporating step kinetics and combined with site balance are solved for the unknown intermediate activities, or site fractions, θ_k. For linear systems, this would result in explicit expressions in terms of ω_ρ, while for nonlinear systems, in general, only numerical results for a given set of conditions (activities of terminal species and temperature) are possible. Once the unknown intermediates surface coverages θ_k are hence evaluated, all the step rates as well as the OR rate can be determined. Additionally, it becomes apparent that all the step rates are simply linear combinations of only μ independent step rates or RR fluxes. It may be noted that this procedure is different from conventional microkinetic analysis, in which θ_k are obtained from a solution of mass balance (partial or ordinary differential) equations of all species in a given reaction system and for a given set of reaction conditions. In fact, for nonlinear kinetic systems, numerical solution of this set of differential equations can be computationally easier than root finding for a set of nonlinear algebraic relations resulting from the corresponding QSS equations.

These hence calculated step rates when written on the RR graph electrical network can quickly reveal which pathways provide the bulk of the flux. Thus, one way to prune the mechanism is to use the RR graph and dropping branches that contribute negligibly to the OR rate, that is $r_\rho / r_{OR} \to 0$, which can often result in clear and drastic pruning. Of course, this needs to be done over a range of conditions of interest to ensure the robustness of the pruned network.

Additionally, once the step rates in the forward direction $\vec{r}_\rho$ and in the reverse direction, $\overleftarrow{r}_\rho$ are determined as above for a given set of conditions, one can readily compute step affinities (Eq. 16) as well as step resistance (Eq. 17), which may also be provided on the RR graph. Steps whose resistance R_ρ is a significant fraction of R_{OR} are kinetically significant and are termed as the RLS, the others are not. In fact, step resistances can be plotted over a broad range of conditions, especially temperature to determine whether the significant steps change. In case there is a step with $R_\rho \to R_{OR}$, it may be denoted as the RDS.

Finally, a comparison of step affinities $\mathcal{A}_\rho$ (or step reversibility, z_ρ, Eq. 16) to those for the OR $\mathcal{A}_{OR}$ (or OR reversibility, z_{OR}), that is, $\mathcal{A}_\rho / \mathcal{A}_{OR}$, also sheds light on which steps are at QE and which are not. Steps with $\mathcal{A}_\rho \to 0$, or with reversibility $z_\rho \to 1$ (Eq. 17), are at QE, while those steps whose $\mathcal{A}_\rho$ is a significant fraction of that of the OR $\mathcal{A}_{OR}$ are the RLSs. Furthermore, it is noteworthy that if there are parallel pathways that contribute significantly to the OR flux, then as per KPL, the affinity drop over all parallel pathways is the same,that is, there are RLSs in all parallel pathways.

An additional possibility is to compare ratio of the power dissipation in each step,[41] namely, $r_\rho \mathcal{A}_\rho$, to that in the OR, $r_{OR}\mathcal{A}_{OR}$

$$\sum_{\rho=1}^{p} \left(\frac{r_\rho \mathcal{A}_\rho}{r_{OR}\mathcal{A}_{OR}} \right) = 1 \tag{19}$$

which stems from the conservation of energy,[41] that is, $\sum_{\rho=1}^{p} r_\rho \mathcal{A}_\rho = r_{OR}\mathcal{A}_{OR}$.

In summary, a comparison of the dissipation as above, along with three different RR graphs labeled with step rates, step affinities, and step resistances can completely illuminate the reaction network, laying bare the important pathways, RLSs, as well as the QE steps. Additionally, plots of step resistances in comparison with that of the OR resistance over a range of temperatures can provide unequivocal evidence of the identity of the crucial steps and pathways in a microkinetic mechanism.

Deriving an Explicit Rate Expression for a Pruned Microkinetic Mechanism. Once the mechanism has been suitably pruned as described above, and the corresponding reduced RR Graph obtained, we have shown[56,57] that an accurate, albeit approximate, explicit rate law may be obtained in the spirit of the LHHW methodology, but following the so-called Rdot approach, even for nonlinear systems, and those with more than one RLSs, for which it is not ordinarily possible to obtain explicit rate expressions. Such explicit rate expressions are, of course, of immense value in the design and analysis of industrial reactors.

The expression for the OR rate takes the form

$$r_{OR} = \frac{(1 - z_{OR})}{R^\bullet_{OR}} = \frac{1}{R^\bullet_{OR}} \left(1 - \frac{1}{K_{OR}} \prod_{i=1}^{n} a_i^{\nu_i} \right) \tag{20}$$

where the overall resistance of the reduced network is computed from its equivalent electrical network in terms of the step Rdots. These in turn are computed from

$$R^\bullet_\rho = \frac{1}{\vec{r}^\bullet_\rho} \tag{21}$$

where the resistance $R^\bullet_\rho$ (Rdot) is equal to the inverse of the rate of the forward step $(1/\vec{r}^\bullet_\rho)$ (Eq. 21), under conditions that it is the RDS, that is, when the entire driving force (affinity) for the OR occurs across it, the other steps being at QE. In other words, step $\vec{r}^\bullet_\rho$ is obtained following the LHHW approach, with which there is broad familiarity and ease.

In short, the step resistances $R^\bullet_\rho$ can be obtained *a priori* via the LHHW methodology, by treating each of the steps as RDS, in turn, and using the QE approximation for the remaining to determine any unknown activities of the intermediate species in $\vec{r}^\bullet_\rho$. The basic idea is that for a given RDS, the q linearly independent unknown intermediate site fractions are determined by identifying the appropriate IRs, or pathways for the formation of intermediates that may be considered to be at QE, that is, all involved steps have $\mathcal{A}_j \to 0$. An IR results from an appropriate

Table 2. Stoichiomteric Numbers for an Example of a Linearly Independent Set of RRs for the WGS Mechanism in Table 1

Cycle	s_2	s_3	s_4	s_5	s_6	s_7	s_8	s_9	s_{10}	s_{11}	s_{12}	s_{13}	s_{14}	s_{15}	s_{16}	OR_1
FR_1	+1	+1	+1	0	0	0	+1	+1	+1	+1	0	0	0	0	0	−1
ER_1	0	0	+1	0	0	0	0	0	0	0	0	0	+1	0	+1	0
ER_2	0	0	0	+1	0	0	0	0	0	0	0	0	+1	−1	0	0
ER_3	0	0	0	0	+1	0	0	0	0	0	0	0	0	−1	−1	0
ER_4	0	0	0	0	0	+1	0	0	−1	0	−1	0	0	0	0	0
ER_5	0	0	0	0	0	0	0	0	0	+1	−1	0	+1	−1	0	0
ER_6	0	0	0	0	0	0	0	0	0	0	−1	+1	0	−1	−1	0

linear combination of steps s_j that eliminates all of the intermediate species except that of interest, I_k, formed from terminal species along with the vacant site S. It is important to pick QE steps s_j that do not violate a KPL relation. For instance, if the RDS s_ρ ($\mathcal{A}_\rho \approx \mathcal{A}_{OR}$) under consideration is a part of an ER, clearly all the steps in the parallel branch of the ER cannot be at QE ($\mathcal{A}_j \to 0$), since that would violate the KPL for the cycle. This is, of course, not true when the cycle contains the OR, for which the affinity drop is equal to $\mathcal{A}_{OR}$.

Finally, the resulting rate law can be further simplified if the surface coverages of some of the intermediates are negligible, as is often the case. In fact, sometimes only a single intermediate is the most abundant reactive intermediate (MARI) on the surface.[27]

Results and Discussion

We will follow the example of the WGS reaction, which we have analyzed before via the RR graph approach,[44] but using a recent DFT microkinetic model for the Pt–Re(111) catalyst.[58] This system with a single OR is not only of great practical significance in a variety of processes but also is one in which the microkinetic models developed are of significant, although not overwhelming, complexity, so that our RR graph-based paring approach can be illustrated meaningfully and without excessive complexity. We will then compare the RR approach to Campbell's DRC for the same mechanism to directly compare the deductions and insights provided by the two alternate approaches.

It should be noted that the mechanism presented cannot be guaranteed to be exhaustive in including all possible steps and intermediates that occur within this system. Our approach evidently does not widen the scope of a mechanism that is proposed through experimentation and DFT calculations, and thus will not be able to suggest what additional steps or intermediates should be included in the mechanism. The major benefits are confirming the consistency of the DFT calculations and the connectivity of the steps, as well as pruning the mechanism down to the steps and kinetics that are most important to driving the reaction in the desired direction.

Constructing the RR graph

The mechanism for the WGS on Pt–Re is shown in Table 1 with $p = 15$ elementary reaction steps s_ρ, and 1 OR. There are a total of 13 unique species which can be divided into $n = 4$ terminal species, that is, the reactants (H_2O and CO) and products (CO_2 and H_2) and, $l = 9$ surface intermediates ($H_2O{\cdot}S$, $CO{\cdot}S$, $H{\cdot}S$, $CO_2{\cdot}S$, $OH{\cdot}S$, $O{\cdot}S$, $COOH{\cdot}S$, $HCOO{\cdot}S$, and S) where S stands for a free active site on the catalyst surface. Due to the site conservation, however, only $q = 8$ out of $l = 9$ intermediates are independent. The RR graph can be constructed based on a complete list of stoichiometrically enumerated RRs and nodes.[56,57] However, this rigorous mathematical enumeration of the complete list of pathways is tedious and unnecessary, as only a handful of RRs are independent.

According to Horiuti–Temkin theorem, only $\mu = p - q = 15 - 8 = 7$ RRs are linearly independent from the complete set of enumerated FRs and ERs for this system. Any appropriate set may be chosen. Additionally, only $\mu - 1 = 7 - 1 = 6$ of the ERs are linearly independent. Thus, a set of seven linearly independent RRs may be readily determined by finding six independent ERs and one FR for the mechanism. These can, in fact, be determined simply from an inspection of the mechanism, thus avoiding the step of systematic stoichiometric algorithm as described in our earlier publications.[41–44,56,57] Such an independent set for this mechanism is provided in Table 2. In fact, the complete set of FRs and ERs can subsequently be determined topologically as walks, once the RR Graph is constructed. A direct FR for this system, as mentioned earlier, involves no more than $q + 1 = 8 + 1 = 9$ elementary steps, and contains no ERs. These FRs and ERs can be enumerated via manual counting or automated graph theoretical tools. This particular system contains 52 unique FRs and 33 unique ERs.

To construct the RR Graph, we begin by drawing the cycle graph by assembling the ERs together such that no reaction step is repeated in the graph by identifying common edges and nodes and fusing these "subgraphs" to produce a cycle graph that includes each ER. For example, in Figure 4a, ER_1 and ER_2 have in common a pair of nodes that have an s_{14} edge between them, so those cycle are fused along that edge.

We continue this process until we have a cycle graph that consists of the six linearly independent ERs. As suggested earlier for this example, each step, including the OR step, should appear twice, and also the graph should be symmetric, which leads to the flipping and doubling of this fused graph (Figure 4b). We can clearly see that the two graphs have two edges (s_6 and s_7) in common that we can fuse to make it symmetrical. We then check each node to make sure that the KFL is satisfied, which are linear combinations of the species QSS relations provided in Table 3. We find the nodes highlighted in Figure 4c to be considered as unbalanced, as they do not satisfy any KFL relation. These nodes can be balanced by adding two s_3 edges to one and two s_8 edges to the other. This creates two new unbalanced nodes to which we can add two s_2 edges and two s_9 edges. The steps s_2, s_3, s_8, and s_9 represent the adsorption and desorption steps that may be placed in any sequential order in the graph without affecting analysis or calculations, but the shown order makes the most sense in terms of how the mechanism proceeds. Finally, the OR is added twice to balance the terminal nodes, resulting in the complete RR graph shown in Figure 2 and its electrical analogy in Figure 3.

Although in this example, we are simply concerned with chemical steps, even surface or pore diffusion steps can be added within the RR graph approach, as illustrated by Deveau et al.[59]

Network Analysis and Pruning. The experimental WGS studies in Ref. 46 were performed on a Pt–Re catalyst primarily at a temperature $T = 548$ K, and pressure $p = 1$ atm, at various feed compositions. For our analysis, we chose parameters

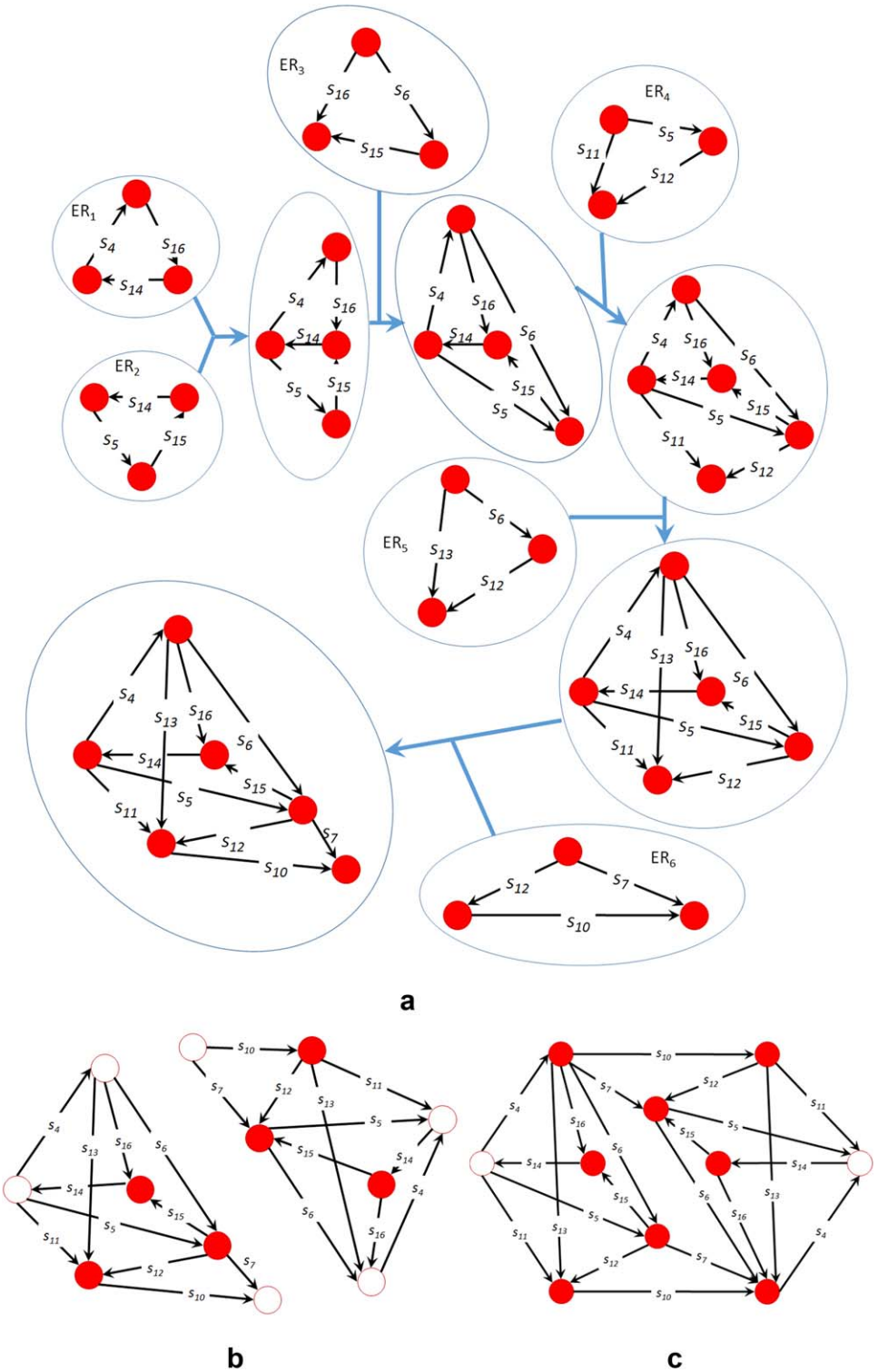

Figure 4. (a) Process of forming the RR graph for the WGS reaction on Pt–Re. ERs are added in succession to form a cycle graph. (b) Original and flipped cycle graphs with unfilled circles representing unbalanced nodes. (c) The two cycle graphs having been merged along s_6 and s_7.

[Color figure can be viewed in the online issue, which is available at wileyonlinelibrary.com.]

similar to those chosen by Carasquillo-Flores et al.,[58] with a feed composition of H_2O (25%), CO (15%), and N_2 (balance), and a conversion, $X = 0.25$. A numerical solution of the KFL equations (QSS relations) for the intermediates concentrations under these conditions was then performed as described in Electrical Analogy and Reaction Networks section. A microkinetic approach based on differential equations was also used to estimate initial values for solving the KFL equations. The step weights ω_ρ for this were determined from terminal species partial pressures and the rate constants determined from the activation energies and pre-exponential factors for the Pt–Re catalyst as tabulated in Table 1.[58] The determination of the intermediates concentrations hence allowed calculation of step rates along with reversibility, affinities, and resistances for the elementary

Table 3. QSS Relations for Each of the Intermediate Species

$Q_{H_2O\cdot S}$:	$(+1)r_2+(-1)r_4+(+1)r_6+(+1)r_{13}+(+1)r_{16}=0$
$Q_{CO\cdot S}$:	$(+1)r_3+(-1)r_7+(-1)r_{10}=0$
$Q_{OH\cdot S}$:	$(+1)r_4+(-1)r_5+(-2)r_6+(-1)r_{10}+(+1)r_{12}+(-1)r_{13}+(+1)r_{15}=0$
$Q_{H\cdot S}$:	$(+1)r_4+(+1)r_5+(-2)r_9+(+1)r_{11}+(-1)r_{14}=0$
$Q_{O\cdot S}$:	$(+1)r_5+(+1)r_6+(-1)r_7+(-1)r_{12}+(-1)\,r_{15}=0$
$Q_{CO_2\cdot S}$:	$(+1)r_7+(-1)r_8+(+1)r_{11}+(+1)r_{12}+(+1)r_{13}+(-1)r_{14}+(+1)r_{15}+(+1)r_{16}=0$
$Q_{COOH\cdot S}$:	$(+1)r_{10}+(-1)r_{11}+(-1)r_{12}+(-1)r_{13}=0$
$Q_{HCOO\cdot S}$:	$(+1)r_{14}+(-1)r_{15}+(-1)r_{16}=0$

reaction steps, which are summarized in Table 4. Finally, the rate of the OR can be obtained from the TNs (Figure 2), for example, $r_{OR}=r_2=r_9$.

It is immediately clear from Figure 2 and Table 4 that there is only one pathway where there is an appreciable flux, while for all other steps and pathways, the flux is negligible. This pathway consists of the adsorption/desorption steps (s_2, s_3, s_8, and s_9), dissociation of water (s_4), formation of carboxyl species (s_{10}), and the subsequent direct dehydrogenation of adsorbed carboxyl (s_{11}). This leads to a reduced RR graph with a single FR (Figure 5), obtained by dropping those with negligible rates.

A look at the calculated resistance of each step for these conditions confirms this conclusion. It further indicates that s_4 and s_{10} have a much higher resistance than the other steps in the remaining FR. Thus, we can approximate the OR rate in terms of the overall resistance being equal to the sum of the resistances of the two steps in sequence, and using Eq. 20

$$r_{OR}=\frac{(1-z_{OR})}{R^{\bullet}_{OR}}=\frac{1}{R^{\bullet}_4+R^{\bullet}_{10}}\left(1-\frac{1}{K_{OR}}\prod_{i=1}^{n}a_i^{\nu_i}\right) \tag{22}$$

The electrical analogy for this is provided in Figure 6.

In short, we can surmise based on this flux analysis and confirmed by the resistance comparisons of the steps, that the FR of $(s_2+s_3+s_4+s_8+s_9+s_{10}+s_{11})$ is the only dominant pathway for the WGS on Pt–Re under these conditions and that steps s_4 and s_{10} can be considered as the two RLSs. This is confirmed for a range of temperatures as shown in Figure 7, which shows an evaluation of the resistances for the steps: s_4, s_{10}, and s_{11}, all others being much smaller.

Explicit Rate Expression through Alternate Form of Ohm's Law. We use the Rdot approach described in *Deriving an Explicit Rate Expression for a Pruned Micro-kinetic Mechanism* section to obtain an explicit rate expression via Eq. 22 for the WGS reaction on the Pt–Re catalyst. For each step, thus, we calculate $R^{\bullet}_p$ by considering each step in turn to be the RDS, the remaining steps being at QE, and then following the conventional LHHW[26,27] approach. This allows determination of the q intermediate site fractions by identifying the appropriate QE IRs, or pathways, for the formation of intermediates. These IRs are found by a linear combination of the QE steps s_j that eliminates all the intermediate species except that of interest, I_k, formed from terminal species along with some reference intermediate, for example, the vacant site S in case of catalytic reactions.

We start by first considering s_4 as the RDS, the remaining steps being at QE. Thus

$$R^{\bullet}_4=\frac{1}{\vec{r}^{\bullet}_4}=\frac{1}{\vec{\omega}_4\theta^{\bullet}_{H_2O\cdot S,4}\theta^{\bullet}_{0,4}}=\frac{1}{\vec{\omega}_4\left(\frac{\theta^{\bullet}_{H_2O\cdot S,4}}{\theta^{\bullet}_{0,4}}\right)(\theta^{\bullet}_{0,4})^2} \tag{23}$$

where the superscript dot refers to the Rdot methodology, and the subscript 4 serves as a reminder that this is for the case when s_4 as the RDS. With all other steps then at QE, appropriate IRs for the formation of the $q=8$ independent surface intermediates, ($H_2O\cdot S$, $CO\cdot S$, $H\cdot S$, $CO_2\cdot S$, $OH\cdot S$, $O\cdot S$, $COOH\cdot S$, and $HCOO\cdot S$) are

$$\begin{gathered}
IR_{H_2O\cdot S}:(+1)s_2\\
IR_{CO\cdot S}:(+1)s_2\\
IR_{OH\cdot S}:\ (-1)s_3+\ (-1)s_5+\ (-1)s_7+\ (-1)s_8+\ (-1/2)s_9\\
IR_{H\cdot S}:\ (-1/2)s_9\\
IR_{O\cdot S}:\ (-1)s_3+\ (-1)s_7+\ (-1)s_8\\
IR_{CO_2\cdot S}:\ (-1)s_8\\
IR_{COOH\cdot S}:\ (-1)s_8+\ (-1/2)s_9+\ (-1)s_{11}\\
IR_{HCOO\cdot S}:(-1)s_5+\ (-1)s_8+\ (-1/2)s_9+\ (-1)s_{15}
\end{gathered} \tag{24}$$

For these steps at QE, the corresponding site fractions, thus, following the LHHW methodology, are

$$\begin{gathered}
\frac{\theta^{\bullet}_{H_2O\cdot S,4}}{\theta^{\bullet}_{0,4}}=\left(\frac{\vec{\omega}_2}{\overleftarrow{\omega}_2}\right)^{+1}\\
\frac{\theta^{\bullet}_{CO\cdot S,4}}{\theta^{\bullet}_{0,4}}=\left(\frac{\vec{\omega}_3}{\overleftarrow{\omega}_3}\right)^{+1}\\
\frac{\theta^{\bullet}_{OH\cdot S,4}}{\theta^{\bullet}_{0,4}}=\left(\frac{\vec{\omega}_3}{\overleftarrow{\omega}_3}\right)^{-1}\left(\frac{\vec{\omega}_5}{\overleftarrow{\omega}_5}\right)^{-1}\left(\frac{\vec{\omega}_7}{\overleftarrow{\omega}_7}\right)^{-1}\left(\frac{\vec{\omega}_8}{\overleftarrow{\omega}_8}\right)^{-1}\left(\frac{\vec{\omega}_9}{\overleftarrow{\omega}_9}\right)^{-1/2}\\
\frac{\theta^{\bullet}_{O\cdot S,4}}{\theta^{\bullet}_{0,4}}=\left(\frac{\vec{\omega}_3}{\overleftarrow{\omega}_3}\right)^{-1}\left(\frac{\vec{\omega}_7}{\overleftarrow{\omega}_7}\right)^{-1}\left(\frac{\vec{\omega}_8}{\overleftarrow{\omega}_8}\right)^{-1}\\
\frac{\theta^{\bullet}_{H\cdot S,4}}{\theta^{\bullet}_{0,4}}=\left(\frac{\vec{\omega}_9}{\overleftarrow{\omega}_9}\right)^{-1/2}\\
\frac{\theta^{\bullet}_{CO_2\cdot S,4}}{\theta^{\bullet}_{0,4}}=\left(\frac{\vec{\omega}_8}{\overleftarrow{\omega}_8}\right)^{-1}\\
\frac{\theta^{\bullet}_{COOH\cdot S,4}}{\theta^{\bullet}_{0,4}}=\left(\frac{\vec{\omega}_8}{\overleftarrow{\omega}_8}\right)^{-1}\left(\frac{\vec{\omega}_9}{\overleftarrow{\omega}_9}\right)^{-1/2}\left(\frac{\vec{\omega}_{11}}{\overleftarrow{\omega}_{11}}\right)^{-1}\\
\frac{\theta^{\bullet}_{HCOO\cdot S,4}}{\theta^{\bullet}_{0,4}}=\left(\frac{\vec{\omega}_5}{\overleftarrow{\omega}_5}\right)^{-1}\left(\frac{\vec{\omega}_8}{\overleftarrow{\omega}_8}\right)^{-1}\left(\frac{\vec{\omega}_9}{\overleftarrow{\omega}_9}\right)^{-1/2}\left(\frac{\vec{\omega}_{15}}{\overleftarrow{\omega}_{15}}\right)^{-1}
\end{gathered} \tag{25}$$

and using site balance to determine the unoccupied site fraction, we finally get

Table 4. Step Resistances, Rates, Reversibilities, and Affinities for Each Step in the WGS Reaction

Reaction Step	Step Resistance	Rate ($s-1$)	Reversibility	Affinity
2	1.15 E − 10	0.0917	1.000	1.05 E − 11
3	1.26 E − 08	0.0917	1.000	1.15 E − 09
4	9.91	0.0917	0.403	9.09 E − 01
5	1.79 E − 07	1.0 E − 06	1.000	1.79 E − 13
6	2.38 E − 11	1.0 E − 07	1.000	2.38 E − 18
7	43.1	1 E − 20	1.000	4.31 E − 19
8	1.55 E − 13	0.0917	1.000	1.42 E − 14
9	7.92 E − 13	0.0917	1.000	7.26 E − 14
10	3.53 E − 01	0.0917	0.968	3.24 E − 02
11	1.56 E − 06	0.0917	1.000	1.43 E − 07
12	5.39 E − 03	1.0 E − 06	1.000	5.39 E − 09
13	4.89 E − 11	1 E − 15	1.000	4.89 E − 26
14	1.08 E − 10	1 E − 14	1.000	1.18 E − 24
15	3.58 E − 10	1 E − 16	1.000	3.58 E − 26
16	2.87 E − 12	1 E − 14	1.000	2.87 E − 26

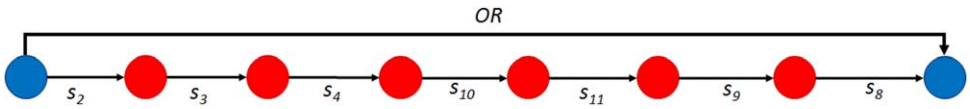

Figure 5. Reduced RR graph for the WGS reaction on Pt–Re catalyst.

[Color figure can be viewed in the online issue, which is available at wileyonlinelibrary.com.]

$$R_4^{\bullet} = \left(\frac{\overleftarrow{\omega}_2}{\vec{\omega}_4\vec{\omega}_2}\right)\left(1+\frac{\vec{\omega}_2}{\overleftarrow{\omega}_2}+\frac{\vec{\omega}_3}{\overleftarrow{\omega}_3}+\frac{\overleftarrow{\omega}_3}{\vec{\omega}_3}\frac{\overleftarrow{\omega}_5}{\vec{\omega}_5}\frac{\overleftarrow{\omega}_7}{\vec{\omega}_7}\frac{\overleftarrow{\omega}_8}{\vec{\omega}_8}\sqrt{\frac{\overleftarrow{\omega}_9}{\vec{\omega}_9}}\right.$$
$$+\frac{\overleftarrow{\omega}_3}{\vec{\omega}_3}\frac{\overleftarrow{\omega}_7}{\vec{\omega}_7}\frac{\overleftarrow{\omega}_8}{\vec{\omega}_8}+\sqrt{\frac{\overleftarrow{\omega}_9}{\vec{\omega}_9}}+\frac{\overleftarrow{\omega}_8}{\vec{\omega}_8}+\frac{\overleftarrow{\omega}_8}{\vec{\omega}_8}\sqrt{\frac{\overleftarrow{\omega}_9}{\vec{\omega}_9}}\frac{\overleftarrow{\omega}_{11}}{\vec{\omega}_{11}} \quad (26)$$
$$\left.+\frac{\overleftarrow{\omega}_5}{\vec{\omega}_5}\frac{\overleftarrow{\omega}_8}{\vec{\omega}_8}\sqrt{\frac{\overleftarrow{\omega}_9}{\vec{\omega}_9}}\frac{\overleftarrow{\omega}_{15}}{\vec{\omega}_{15}}\right)^2$$

Performing a similar analysis for $R_{10}^{\bullet}$, that is, with step s_{10} as the RDS

$$R_{10}^{\bullet} = \left(\frac{\overleftarrow{\omega}_2\overleftarrow{\omega}_3\overleftarrow{\omega}_4}{\vec{\omega}_{10}\vec{\omega}_2\vec{\omega}_3\vec{\omega}_4}\sqrt{\frac{\overleftarrow{\omega}_9}{\vec{\omega}_9}}\right)$$
$$\left(1+\frac{\vec{\omega}_2}{\overleftarrow{\omega}_2}+\frac{\vec{\omega}_3}{\overleftarrow{\omega}_3}+\frac{\overleftarrow{\omega}_2}{\vec{\omega}_2}\frac{\overleftarrow{\omega}_4}{\vec{\omega}_4}\sqrt{\frac{\overleftarrow{\omega}_9}{\vec{\omega}_9}}+\frac{\overleftarrow{\omega}_3}{\vec{\omega}_3}\frac{\overleftarrow{\omega}_7}{\vec{\omega}_7}\frac{\overleftarrow{\omega}_8}{\vec{\omega}_8}\right. \quad (27)$$
$$\left.+\sqrt{\frac{\overleftarrow{\omega}_9}{\vec{\omega}_9}}+\frac{\overleftarrow{\omega}_8}{\vec{\omega}_8}+\frac{\overleftarrow{\omega}_8}{\vec{\omega}_8}\sqrt{\frac{\overleftarrow{\omega}_9}{\vec{\omega}_9}}\frac{\overleftarrow{\omega}_{11}}{\vec{\omega}_{11}}+\frac{\overleftarrow{\omega}_5}{\vec{\omega}_5}\frac{\overleftarrow{\omega}_8}{\vec{\omega}_8}\sqrt{\frac{\overleftarrow{\omega}_9}{\vec{\omega}_9}}\frac{\overleftarrow{\omega}_{15}}{\vec{\omega}_{15}}\right)^2$$

By examining each site fraction individually, that is, $\frac{\theta_{k,p}^{\bullet}}{\theta_{0,p}^{\bullet}}$, it is possible to simplify these further.[27] Thus, $\frac{\theta_{H_2O\cdot S}^{\bullet}}{\theta_{0,p}^{\bullet}}=0.113$, $\frac{\theta_{CO\cdot S}^{\bullet}}{\theta_{0,p}^{\bullet}}=0.644$, $\frac{\theta_{OH\cdot S}^{\bullet}}{\theta_{0,p}^{\bullet}}=0.000131$, $\frac{\theta_{O\cdot S}^{\bullet}}{\theta_{0,p}^{\bullet}}=0.000685$, $\frac{\theta_{H\cdot S}^{\bullet}}{\theta_{0,p}^{\bullet}}=0.194$, $\frac{\theta_{CO_2\cdot S}^{\bullet}}{\theta_{0,p}^{\bullet}}=0.000150$, $\frac{\theta_{COOH\cdot S}^{\bullet}}{\theta_{0,p}^{\bullet}}=0.0000445$, and $\frac{\theta_{HCOO\cdot S}^{\bullet}}{\theta_{0,p}^{\bullet}}=0.00000315$, which reveals that $\theta_{O\cdot S}^{\bullet}$,$\theta_{COOH\cdot S}^{\bullet}$,$\theta_{OH\cdot S}^{\bullet}$,$\theta_{CO_2\cdot S}^{\bullet}$, and $\theta_{HCOO\cdot S}^{\bullet}$ are relatively insignificant in comparison to $\theta_{CO\cdot S}^{\bullet}$,$\theta_{H_2O\cdot S}^{\bullet}$, and $\theta_{H\cdot S}^{\bullet}$ in both $R_4^{\bullet}$ and $R_{10}^{\bullet}$, so that the smaller site fractions can be neglected when summing the site fractions to find $\theta_{0,p}^{\bullet}$. Thus, the above expressions simplify to

$$R_4^{\bullet} \approx \left(\frac{\overleftarrow{\omega}_2}{\vec{\omega}_4\vec{\omega}_2}\right)\left(1+\frac{\vec{\omega}_2}{\overleftarrow{\omega}_2}+\frac{\vec{\omega}_3}{\overleftarrow{\omega}_3}+\sqrt{\frac{\overleftarrow{\omega}_9}{\vec{\omega}_9}}\right)^2 \quad (28)$$

and

$$R_{10}^{\bullet} \approx \left(\frac{\overleftarrow{\omega}_2\overleftarrow{\omega}_3\overleftarrow{\omega}_4}{\vec{\omega}_{10}\vec{\omega}_2\vec{\omega}_3\vec{\omega}_4}\sqrt{\frac{\overleftarrow{\omega}_9}{\vec{\omega}_9}}\right)\left(1+\frac{\vec{\omega}_2}{\overleftarrow{\omega}_2}+\frac{\vec{\omega}_3}{\overleftarrow{\omega}_3}+\sqrt{\frac{\overleftarrow{\omega}_9}{\vec{\omega}_9}}\right)^2 \quad (29)$$

so that the simplified expression for the overall rate from Eqs. 22, 28, and 29

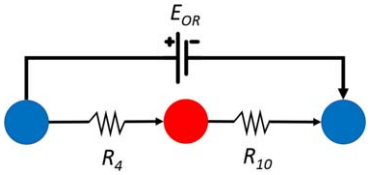

Figure 6. Simplified electrical analogy diagram for the WGS reaction on Pt–Re catalyst.

[Color figure can be viewed in the online issue, which is available at wileyonlinelibrary.com.]

$$r_{OR} \approx \frac{1}{\left(1+\frac{\overleftarrow{\omega}_3\overleftarrow{\omega}_4}{\vec{\omega}_{10}\vec{\omega}_3}\sqrt{\frac{\overleftarrow{\omega}_9}{\vec{\omega}_9}}\right)\frac{\overleftarrow{\omega}_2}{\vec{\omega}_4\vec{\omega}_2}\left(1+\frac{\vec{\omega}_2}{\overleftarrow{\omega}_2}+\frac{\vec{\omega}_3}{\overleftarrow{\omega}_3}+\sqrt{\frac{\overleftarrow{\omega}_9}{\vec{\omega}_9}}\right)^2} \quad (30)$$
$$\left(1-\frac{1}{K_{OR}}\frac{p_{CO_2}p_{H_2}}{p_{H_2O}p_{CO}}\right)$$

Finally, substituting the rate constants and concentration of terminal species for reaction step weights ω_p (Table 1), we have the OR rate expression in the conventional form

$$r_{OR} \approx \frac{\vec{k}_4\vec{k}_{10}K_2K_3\sqrt{K_9}^9 p_{H_2O}p_{CO}}{\left(\vec{k}_{10}K_3\sqrt{K_9}p_{CO}+\overleftarrow{k}_4\sqrt{p_{H_2}}\right)\left(1+K_2p_{H_2O}+K_3p_{CO_2}+\sqrt{\frac{1}{K_9p_{H_2}}}\right)^2} \quad (31)$$
$$\left(1-\frac{1}{K_{OR}}\frac{p_{CO_2}p_{H_2}}{p_{H_2O}p_{CO}}\right)$$

where, $K_\rho=\vec{k}_\rho/\overleftarrow{k}_\rho$ is the equilibrium constant for step s_p, and the DFT parameters for the rate constants are provided in Table 1.

This equation is in good agreement with the results of the numerically calculated QSS calculation as shown in a parity plot (Figure 8), proving that the Rdot method and subsequent simplifications are valid for the kinetic data (Table 1) employed for the WGS reaction on Pt–Re catalyst.

Analysis via Campbell's DRC

Campbell's DRC analysis for the WGS reaction on Pt–Re catalyst was conducted from the rates for each step calculated via numerical QSS analysis for the same conditions used in the previous section, that is, a temperature of 548 K, and pressure $p = 1$ atm with a feed composition of H_2O (25%), CO

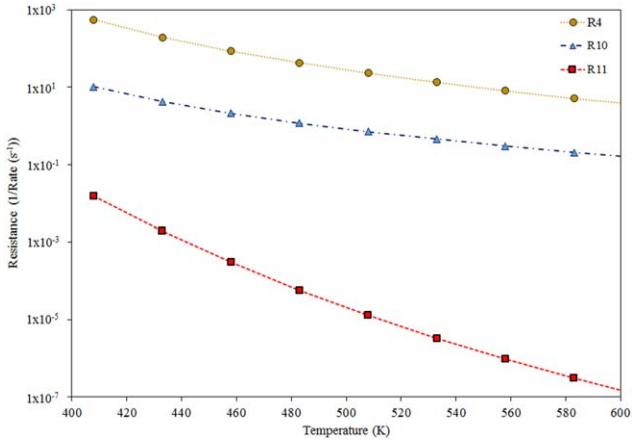

Figure 7. Comparison of step resistances R_i for the nonadsorption/desorption steps vs. temperature for the dominant pathway of the WGS reaction on Pt–Re.

[Color figure can be viewed in the online issue, which is available at wileyonlinelibrary.com.]

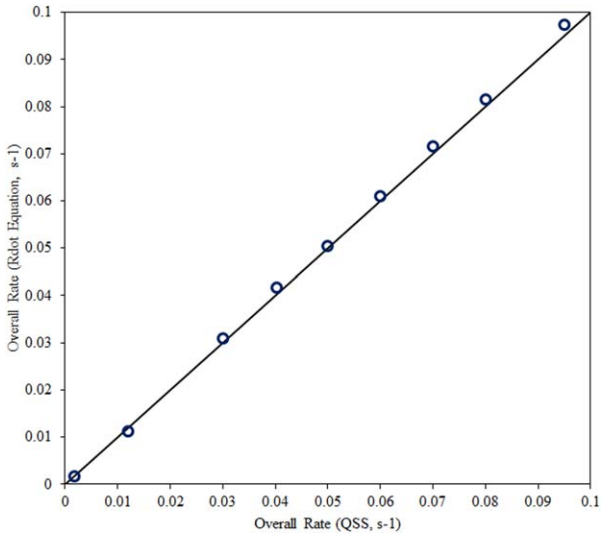

Figure 8. Comparison of overall QSS rate obtained from implementation of Ohm's law Eq. 32 and that calculated numerically for the WGS reaction on Pt–Re, where each point is a different temperature for which the QSS rate is calculated.

[Color figure can be viewed in the online issue, which is available at wileyonlinelibrary.com.]

(15%), and N_2 (balance), and a conversion, $X = 0.25$. To estimate $X_{\mathrm{DRC},\rho}$(Eq. 6 or 9), the change in the overall rate when a rate constant changes incrementally was calculated as follows. The forward rate constant of a chosen step was thus increased by a small amount (i.e., 1%), and as $K_\rho = \vec{k}_\rho / \overleftarrow{k}_\rho$ needs to be constant, the reverse rate constant was increased by 1% as well. The new r_{OR} was calculated using the increased $\vec{k}_\rho$ and $\overleftarrow{k}_\rho$ values, with all other rate constants remaining unchanged. Thus, the Campbell's DRC was calculated using the finite difference form of Eq. 6

$$X_{\mathrm{DRC},\rho} \approx \frac{\vec{k}_\rho}{r_{\mathrm{OR}}} \cdot \left(\frac{\Delta r_{\mathrm{OR}}}{\Delta \vec{k}_\rho} \right)_{\mathbf{a}, k_{r \neq \rho}} \tag{32}$$

This process was completed for each step of the mechanism in turn and compared to the analogous calculations for this system reported by Carrasquillo-Flores et al.[58] (Table 5). The results are similar, showing that s_{10}, the formation of the carboxyl species step, has the largest DRC and is hence the RDS, the DRC of all other steps being insignificant or zero.

A similar approach was used to estimate Campbell's DTC, as given in Eq. 11, to determine the significance of the stability of an intermediate species on OR rate. For numerical estimation, we used the finite difference form of Eq. 11. As changing the GFE of formation directly changes the binding energy, to calculate Campbell's DTC for an intermediate k, the binding energy of that intermediate was reduced by 1% while all other binding energies were kept constant. The rate constants for each forward or reverse reaction step that includes that intermediate was thus changed due to the activation energy barrier being raised due to the lower energy state of the intermediate. The above described QSS numerical calculation was then performed using these new rate constants to find the change in the overall rate. This was repeated for each of the eight intermediates and the results are shown in Table 6.

Table 5. Values for Campbell's Degree of Rate Control for Pt–Re Catalyst for [1] This Work and [2] Carrasquillo-Flores et al.[58]

Reaction Step	$X^{[1]}_{\mathrm{DRC,Pt–Re}}$	$X^{[2]}_{\mathrm{RC,Pt–Re}}$
1	0	0
2	0	0
3	0	0
4	-1×10^{-4}	-3×10^{-4}
5	0	0
6	0	0
7	0	0
8	0	0
9	0	0
10	0.95	0.95
11	8×10^{-3}	9×10^{-3}
12	0	0
13	0	0
14	0	0
15	0	0
16	0	0

Carasquillo-Flores et al. reported coverage of CO to be approximately 2/3 ML and coverage of H atoms to range between 0.15 and 0.2 ML under similar conditions for their model.[58] This agrees with the results for both Campell's DRC and the RR graph approach. As seen in Table 6, $X_{\mathrm{DTC,CO}} = -0.65$ and $X_{\mathrm{DTC,H}} = -0.058$, which suggests that CO is the MARI for these conditions with some H atoms also occupying the surface. The site fraction comparison for the Rdot method also suggest that CO is the MARI for this reaction with H coverage having additional, although lesser, importance.

Comparison of Campbell's DRC and RR graph approach

For the example of WGS reaction on the Pt–Re catalyst, Campbell's DRC determines that the formation of the carboxyl species step (s_{10}) is the RDS of the mechanism, as its $X_{\mathrm{DRC},10} = 0.96$, that for the remaining steps being much smaller or zero. Conversely, the RR approach concludes that the dissociation of water step (s_4) is the largest contributor to limiting the overall rate, with s_{10} also limiting the rate somewhat, although not to the same extent as s_4. Carrasquillo-Flores et al.,[58] in fact, also eventually concluded that s_4 was the RDS despite s_{10} being indicated as the RDS from Campbell's DRC, stating: "Putting all the observations together we infer that H_2O activation, s_4, is the underlying rate-controlling step."

Carrasquillo-Flores et al.[58] further noted that based on their model and experiments, they concluded that the pathway including s_4, s_{10}, and s_{11} was the only pathway with a significant amount of flux. Not only does the RR approach agree

Table 6. Values for Campbell's Degree of Thermodynamic Control for Each Reaction Intermediate

Reaction Intermediate	$X_{\mathrm{DTC,Pt–Re}}$
O·S	0
OH·S	0
CO·S	−0.650
CO_2·S	−0.018
COOH·S	0
H_2O·S	0
H·S	−0.058
HCOO·S	0

with this conclusion arrived at circuitously by the authors but also it provides a quantitative estimation of how much each step contributes to the overall rate. Clearly, Campbell's DRC arrives at the wrong conclusion in this case.

Furthermore, according to Campbell's theory, the sum of the DRC of all the steps should add to unity. For the WGS reaction on Pt–Re catalyst, it is found to be 0.96, which is close to, but not precisely unity. However, there are examples that show that it is significantly different from unity. Thus, according to the results found in Ref. 25 for the WGS reaction on Cu catalyst, it only adds up to approximately 0.83, well below unity. Conversely, this does not seem to affect the conclusions one can make about a mechanism, as long as for one of the steps $X_{\mathrm{DRC},\rho}$ is much higher than that of any other step.

For the WGS reaction example under consideration, thus, there is more than one RLS and this conclusion does not much change with temperature (see Figure 7) or other conditions. In fact, the RR approach provides quantitative estimates of the resistance of each step and clearly identifies those that limit the rate and the pathways that contribute significantly, along with a robust rate law.

Conclusions

We have shown via a detailed example of how the analysis and reduction of a reaction mechanism can be accomplished using the electrical network analogy within our RR graph method. Although Campbell's DRC is the most common technique available, currently, we show here that our RR graph approach is superior and more insightful. The example of the WGS reaction on Pt–Re considered here, in fact, shows that Campbell's DRC can lead to erroneous conclusions that are inconsistent with experimental results.[58] Further, the contention that $\sum_{\rho=1}^{p} X_{\mathrm{DRC},\rho}=1$ is not true in general. The RR graph method is not limited to single RDS or single pathway mechanisms in its usefulness. Furtherz, the electrical analogy combined with the well-familiar LHHW methodology provides accurate rate expressions even for *nonlinear* cases such as the WGS reaction example considered here, not otherwise possible. It may thus be concluded that the electrical analogy and the RR graph approach is a much more effective and revealing Ockham's razor for pruning microkinetic catalytic mechanisms than is Cambell's DRC.

A current limitation of our approach is that manually drawing the RR graph for a system with a very large number of steps is challenging, especially for nonlinear systems such as the WGS reaction. However, this does not limit the efficacy of the electrical analogy approach in pruning a large mechanism via a comparison of the computed reaction step resistance and affinity following a numerical QSS analysis. This is just similar to performing a numerical circuit analysis without the benefit of a wiring diagram. Of course, we envision a tool that will eventually automate the graph drawing process.

Notation

Symbols

a_i = activity of terminal species i
A_ρ = affinity of elementary reaction ρ
$\mathcal{A}_\rho$ = a dimensionless reaction affinity of elementary reaction ρ
$\mathcal{A}_{\mathrm{OR}}$ = a dimensionless affinity of the overall reaction
$\mathcal{A}_{\mathrm{IR}}$ = a dimensionless affinity of intermediate reaction
BE_{I_k} = binding energy of intermediate species, I_k
$\vec{E}_\rho$ = activation energy of the forward reaction
$\overleftarrow{E}_\rho$ = activation energy of the reverse reaction
ΔG_ρ = Gibbs free energy change of the elementary reaction ρ
$G_\rho^{\ddagger,\mathrm{o}}$ = Gibbs-free energy of activation
G_f^{o} = standard enthalpy of formation in the gas phase
$H_{I_k(g)}^{\mathrm{o}}$ = standard enthalpy of formation in the adsorbed intermediate
$\Delta H_\rho^{\ddagger,\mathrm{o}}$ = enthalpy of activation
h = Planck's constant
I_k = intermediate species k
K_ρ = equilibrium constant of the elementary reaction ρ
K_{OR} = equilibrium constant of the overall reaction
$\vec{k}_\rho$ = forward rate constant of the elementary reaction ρ
$\overleftarrow{k}_\rho$ = backward rate constant of the elementary reaction ρ
k_{B} = Boltzman's constant
n = number of terminal species
N_{Av} = Avogadro's number
p = number of elementary reactions
p_i = partial pressure of species i
q = number of linearly independent intermediate species
R = gas constant
R_ρ = resistance of elementary reaction ρ
$R_\rho^\bullet$ = resistance of elementary reaction s_ρ, when s_ρ is the RDS
R_{OR} = total resistance of the overall reaction network
r_ρ = net rate of the elementary reaction ρ
r_{OR} = net rate of the overall reaction
$\vec{r}_\rho$ = forward rate of elementary reaction ρ
$\overleftarrow{r}_\rho$ = reverse rate of elementary reaction ρ
$\vec{r}_\rho^{\,\bullet}$ = maximum forward rate of the elementary reaction ρ
$\overleftarrow{r}_\rho^{\,\bullet}$ = maximum reverse rate of the elementary reaction ρ
S = unoccupied surface site
ΔS_ρ = entropy change the elementary reaction ρ
$\Delta \vec{S}_\rho^{\ddagger,\mathrm{o}}$ = entropy of activation
s_ρ = elementary reaction ρ
T = temperature
T_i = terminal species i
$X_{\mathrm{DRC},\rho}$ = degree of rate control of step s_ρ
$X_{\mathrm{DTC},\rho}$ = degree of thermodynamic control of step s_ρ
z_ρ = reversibility of reaction s_ρ
z_{OR} = reversibility of overall reaction
z_{IR} = reversibility of an intermediate reaction

Greek symbols

β_ρ = symmetry factor
ρ = elementary reaction
σ_ρ = stoichiometric number for the elementary reaction ρ in a RR
Λ_ρ = pre-exponential factor
θ_k = surface coverage of intermediate species k
$\theta_{k,\rho}^\bullet$ = surface coverage of intermediate species k when step ρ is the RDS
μ = number of linearly independent reaction routes
ω_ρ = step weight for reaction ρ
$\vec{\omega}_\rho$ = forward step weight for reaction ρ
$\overleftarrow{\omega}_\rho$ = reverse step weight for reaction ρ
ν_i = stoichiometric coefficient of terminal species i in an overall reaction
$\nu_{\rho i}$ = stoichiometric coefficient of species i in reaction ρ

Abbreviations

DFT = density functional theory
DRC = degree of rate control
DTC = degree of thermodynamic control
EMF = electromotive force
ER = empty route
FR = full route
GFE = Gibbs free energy
IN = intermediate node
IR = intermediate reaction
KFL = Kirchhoff's flux (node) law
KPL = Kirchhoff's potential (loop) law
LHHW = Langmuir–Hinshelwood–Hougen–Watson
MARI = most abundant reactive intermediate
OR = overall reaction
QSS = quasi-steady state
QE = quasi-equilibrium
RR = reaction route
RDS = rate-determining step
RLS = rate-limiting step

TN = terminal node
TTST = thermodynamic transition-state theory
WGS = water–gas shift

Literature Cited

1. Dumesic JA, Rudd DF, Aparicio LM, Rekoske JE, Treviño AA. *The Microkinetics of Heterogeneous Catalysis*. Washington, DC: American Chemical Society, 1993.
2. Ertl G. Heterogeneous catalysis on the atomic scale. *Chem Rec*. 2001;1(1):33–45.
3. Cortright RD, Dumesic JA. Kinetics of heterogeneous catalytic reactions: analysis of reaction schemes. *Adv Catal*. 2001;46:161–264.
4. Dumesic JA, Huber GW, Boudart M. Principles of heterogeneous catalysis. In: *Handbook of Heterogeneous Catalysis*, Weinheim: Wiley-VCH, 2008.
5. Law CK, Sung CJ, Wang H, Lu TF. Development of comprehensive detailed and reduced reaction mechanisms for combustion modeling. *AIAA J*. 2003;41(9):1629–1646.
6. Li J, Zhao Z, Kazakov A, Dryer FL. An updated comprehensive kinetic model of hydrogen combustion. *Int J Chem Kinet*. 2004; 36(10):566–575.
7. Kee RJ, Coltrin ME, Glarborg P. *Chemically Reacting Flow: Theory and Practice*. Hoboken, NJ: Wiley, 2005.
8. Pandis SN, Seinfeld JH. Sensitivity analysis of a chemical mechanism for aqueous-phase atmospheric chemistry. *J Geophys Res: Atmos (1984–2012)*. 1989;94(D1):1105–1126.
9. Gao D, Stockwell WR, Milford JB. First-order sensitivity and uncertainty analysis for a regional-scale gas-phase chemical mechanism. *J Geophys Res: Atmos (1984–2012)*. 1995;100(D11):23153–23166.
10. Sandu A, Daescu DN, Carmichael GR, Chai T. Adjoint sensitivity analysis of regional air quality models. *J Comput Phys*. 2005;204(1): 222–252.
11. Degenring D, Froemel C, Dikta G, Takors R. Sensitivity analysis for the reduction of complex metabolism models. *J Process Control*. 2004;14(7):729–745.
12. Smith GP, Golden DM, Frenklach M, Moriarty NW, Eiteneer B, Goldenberg M, Bowman CT, Hanson RK, Song S, Gardiner WC Jr, Lissianski VV, Qin Z. GRI-Mech—An Optimized Detailed Chemical Reaction Mechanism for Methane Combustion, 1999. Available at: http://www.me.berkeley.edu/gri_mech/
13. Mhadeshwar AB, Vlachos DG. Is the water–gas shift reaction on Pt simple? Computer-aided microkinetic model reduction, lumped rate expression, and rate-determining step. *Catal Today*. 2005;105(1): 162–172.
14. Sutton JE, Panagiotopoulou P, Verykios XE, Vlachos DG. Combined DFT, microkinetic, and experimental study of ethanol steam reforming on Pt. *J Phys Chem*. 2013;117(9):4691–4706.
15. Farberow CA, Dumesic JA, Mavrikakis M. Density functional theory calculations and analysis of reaction pathways for reduction of nitric oxide by hydrogen on Pt (111). *ACS Catal*. 2014;4:3307.
16. Heyden A, Hansen N, Bell AT, Keil FJ. Nitrous oxide decomposition over Fe-ZSM-5 in the presence of nitric oxide: a comprehensive DFT study. *J Phys Chem B*. 2006;110(34):17096–17114.
17. Broadbelt LJ, Snurr RQ. Applications of molecular modeling in heterogeneous catalysis research. *Appl Catal A*. 2000;200(1):23–46.
18. Gokhale AA, Kandoi S, Greeley JP, Mavrikakis M, Dumesic JA. Molecular-level descriptions of surface chemistry in kinetic models using density functional theory. *Chem Eng Sci*. 2004;59(22):4679–4691.
19. Nørskov JK, Abild-Pedersen F, Studt F, Bligaard T. Density functional theory in surface chemistry and catalysis. *Proc Natl Acad Sci USA*. 2011;108(3):937–943.
20. Shustorovich E, Sellers H. The UBI-QEP method: a practical theoretical approach to understanding chemistry on transition metal surfaces. *Surf Sci Rep*. 1998;31(1):1–119.
21. Fishtik I, Datta R. A UBI–QEP microkinetic model for the water–gas shift reaction on Cu (111). *Surf Sci*. 2002;512(3):229–254.
22. Waugh KC. Prediction of global reaction kinetics by solution of the arrherius parametrized component elementary reactions: microkinetic analysis. *Catal Today*. 1999;53:161–176.
23. Stoltze P. Microkinetic simulation of catalytic reactions. *Prog Surf Sci*. 2000;65(3):65–150.
24. Lynggaard H, Andreasen A, Stegelmann C, Stoltze P. Analysis of simple kinetic models in heterogeneous catalysis. *Prog Surf Sci*. 2004;77(3):71–137.
25. Madon RJ, Braden D, Kandoi S, Nagel P, Mavrikakis M, Dumesic JA. Microkinetic analysis and mechanism of the water gas shift reaction over copper catalysts. *J Catal*. 2011;281(1):1–11.
26. Hougen OA, Watson KM. Solid catalysts and reaction rates—general principles. *Ind Eng Chem*. 1943;35:529–541.
27. Boudart M, Djéga-Mariadassou G. *Kinetics of Heterogeneous Catalytic Reactions*. Princeton, NJ: Princeton University Press, 1984.
28. Boudart M. From the century of the rate equations to the century of the rate constants: a revolution in catalytic kinetics and assisted catalyst design. *Catal Lett*. 2000;65:1–3.
29. Hoffmann R, Minkin VI, Carpenter BK. Ockham's razor and chemistry. *Bull Soc Chim Fr*. 1996;133(2):117–130.
30. Lu T, Law CK. A criterion based on computational singular perturbation for the identification of quasi steady state species: a reduced mechanism for methane oxidation with NO chemistry. *Combust Flame*. 2008;154(4):761–774.
31. Zhang H, Linford JC, Sandu A, Sander R. Chemical mechanism solvers in air quality models. *Atmosphere*. 2011;2(3):510–532.
32. Nørskov JK, Bligaard T, Rossmeisl J, Christensen CH. Towards the computational design of solid catalysts. *Nat Chem*. 2009;1(1):37–46.
33. Dumesic JA. Analyses of reaction schemes using De Donder relations. *J Catal*. 1999;185(2):496–505.
34. Campbell CT. Future directions and industrial perspectives micro- and macro-kinetics: their relationship in heterogeneous catalysis. *Top Catal*. 1994;1(3–4):353–366.
35. Campbell CT. Finding the rate-determining step in a mechanism: comparing DeDonder relations with the "Degree of Rate Control." *J Catal*. 2001;204(2):520–524.
36. Stegelmann C, Andreasen A, Campbell CT. Degree of rate control: how much the energies of intermediates and transition states control rates. *J Am Chem Soc*. 2009;131(23):8077–8082.
37. Nørskov JK, Bligaard T, Kleis J. Rate control and reaction engineering. *Science*. 2009;24(5935):1655.
38. Dumesic JA. Reply to finding the rate-determining step in a mechanism: comparing DeDonder relations with the "Degree of Rate Control." *J Catal*. 2001;204:525–529.
39. Varma A, Morbidelli M, Wu H. *Parametric sensitivity in chemical systems*. Cambridge: Cambridge University Press, 2005.
40. Mhadeshwar AB, Vlachos DG. Hierarchical multiscale mechanism development for methane partial oxidation and reforming and for thermal decomposition of oxygenates on Rh. *J Phys Chem B*. 2005; 109(35):16819–16835.
41. Fishtik I, Callaghan CA, Datta R. Reaction route graphs. I. Theory and algorithm. *J Phys Chem B*. 2004;108(18):5671–5682.
42. Fishtik I, Callaghan CA, Datta R. Reaction route graphs. II. Examples of enzyme- and surface-catalyzed single overall reactions. *J Phys Chem B*. 2004;108(18):5683–5697.
43. Fishtik I, Callaghan CA, Datta R. Reaction route graphs. III. Nonminimal kinetic mechanisms. *J Phys Chem B*. 2005;109(7):2710–2722.
44. Callaghan CA, Vilekar SA, Fishtik I, Datta R. Topological analysis of catalytic reaction networks: water gas shift reaction on Cu (111). *Appl Catal A*. 2008;345(2):213–232.
45. Meskine H, Matera S, Scheffler M, Reuter K, Metiu H. Examination of the concept of degree of rate control by first-principles kinetic Monte Carlo simulations. *Surf Sci*. 2009;603(10):1724–1730.
46. Bendtsen AB, Glarborg P, Dam-Johansen K. Visualization methods in analysis of detailed chemical kinetics modeling. *Comput Chem*. 2001;25(2):161–170.
47. Vajda S, Valko P, Turanyi T. Principal component analysis of kinetic models. *Int J Chem Kinet*. 1985;17(1):55–81.
48. Turanyi T, Berces T, Vajda S. Reaction rate analysis of complex kinetic systems. *Int J Chem Kinet*. 1989;21(2):83–99.
49. Barański A. On the usefulness of Campbell's concept of the rate-determining step. *Solid State Ionics*. 1999;117(1):123–128.
50. Connors KA. *Chemical Kinetics: The Study of Reaction Rates in Solution*. New York: Wiley-VCH, 1990.
51. Bligaard T, Nørskov JK, Dahl S, Matthiesen J, Christensen CH, Sehested J. The Brønsted–Evans–Polanyi relation and the volcano curve in heterogeneous catalysis. *J Catal*. 2004;224(1):206–217.
52. Boudart M, Tamaru K. The step that determines the rate of a single catalytic cycle. *Catal Lett*. 1991;9(1–2):15–22.
53. Happel J, Sellers PH. Analysis of the possible reaction mechanisms for a chemical reaction system. *Adv Catal*. 1983;32:273–323.
54. Milner PC. The possible mechanisms of complex reactions involving consecutive steps. *J Electrochem Soc*. 1964;3:228–232.
55. Chua LO, Desoer CA, Kuh ES. *Linear and Nonlinear Circuits*. New York: McGraw Hill, 1987.

56. Vilekar SA, Fishtik I, Datta R. The steady-state kinetics of a catalytic reaction sequence. *Chem Eng Sci*. 2009;64(9):1968–1979.
57. Vilekar SA, Fishtik I, Datta R. The steady-state kinetics of parallel reaction networks. *Chem Eng Sci*. 2010;65(10):2921–2933.
58. Carrasquillo-Flores R, Gallo JMR, Hahn K, Dumesic JA, Mavrikakis M. Density functional theory and reaction kinetics studies of the water–gas shift reaction on Pt–Re catalysts. *ChemCatChem*. 2013; 5(12):3690–3699.
59. Deveau ND, Ma YH, Datta R. Beyond Sieverts' law: a comprehensive microkinetic model of hydrogen permeation in dense metal membranes. *J Membr Sci*. 2013;437:298–311.

Manuscript received Mar. 11, 2015, and revision received June 23, 2015.